NIH Public Access
Author Manuscript
Medchemcomm. Author manuscript; available in PMC 2012 February 1.

Published in final edited form as:
Medchemcomm. 2012 ; 3(2): 179–194. doi:10.1039/C1MD00232E.

Syntheses and properties of trimethylaminophenoxy-substituted Zn(II)-phthalocyanines†

Benson G. Ongarora, **Xiaoke Hu**, **Hairong Li**, **Frank R. Fronczek**, and **M. Graça H. Vicente***
Department of Chemistry, Louisiana State University, Baton Rouge, LA 70803, USA

Abstract

The syntheses, photophysical properties and in vitro biological behavior of a series of nine Zn(II)-phthalocyanines (ZnPcs) bearing one to eight positively-charged trimethylaminophenoxy groups are reported. All ZnPcs are highly soluble in polar organic solvents, and show fluorescence and singlet oxygen quantum yields in the ranges 0.11–0.21 and 0.16–0.47, respectively. The cytotoxicity of the ZnPcs depends on both the number of charges and their site of substitution (α vs. β) on the Pc isoindole units; the most promising for PDT application are the α-substituted di-cationic ZnPcs **6a** and **17a**.

Introduction

Photodynamic therapy (PDT) combines a porphyrin-based photosensitizer (PS), visible light and oxygen to promote selective destruction of malignant tissue *via* the generation of reactive oxygen species (ROS).[1,2] Upon light activation, usually from a laser, the PS produces an excited triplet state *via* intersystem crossing from a short-lived excited singlet state, which reacts with biomolecules and/or molecular oxygen generating ROS.[3] Highly transient singlet oxygen is believed to be the main cytotoxic species formed in PDT. Since the ROS, and in particular singlet oxygen, have short lifetimes *in vivo* (on the order of μs) and limited travel paths in tissues, the site of their generation is crucial to the PDT therapeutic outcome.[3–6] Two porphyrin derivatives, Photofrin and Visudyne, are currently FDA-approved for the PDT treatment of melanoma, early and advanced stage cancer of the lung, digestive tract, genitourinary tract, Barret's esophagus and, in the latter case, the wet form of age-related macular degeneration.[4,5] The minimally invasive nature of PDT, normally involving the systemic administration of the PS and fiber optic light delivery, make it highly attractive for the treatment of localized tumors and other non-malignant conditions in dermatology, ophthalmology and cardiology.

Although Photofrin has been successfully used in the treatment of thousands of patients worldwide, it has some drawbacks in that it is a complex mixture of compounds, has limited tissue selectivity and absorbs only weakly in the red region of the spectrum (λ_{max} = 630 nm) where light penetrates deeper into tissues. Therefore intense research in the last decades has focused on the development of PS with improved targeted tissue selectivity and overall PDT efficacy compared with Photofrin. Among these, phthalocyanines (Pcs) are particularly promising 2 second-generation PS due to their long wavelength absorptions in the infra-red region of the spectrum with high extinction coefficients, high photochemical stability and

†Electronic supplementary information (ESI) available: Absorption and emission figures for all cationic ZnPcs in DMF and in PBS at pH = 7.4. CCDC reference numbers 810389 and 835347. For ESI and crystallographic data in CIF or other electronic format see DOI: 10.1039/c1md00232e

This journal is © The Royal Society of Chemistry 2011

vicente@lsu.edu; Fax: +1 225 578 3458; Tel: +1 225 578 7405.

NIH-PA Author Manuscript
NIH-PA Author Manuscript
NIH-PA Author Manuscript

NIH-PA Author Manuscript

NIH-PA Author Manuscript

NIH-PA Author Manuscript

superior ability for generation of singlet oxygen.[7–9] The amphiphilicity of Pc derivatives can be tuned *via* the attachment of various water-solubilizing and/or bulky groups to either the macrocycle periphery or its center core. Such substitution can at least in part overcome their well-known aggregation behavior in solutions, thus improving their quantum yields and photodynamic efficacy.[9]

Among the substituted Pcs, positively charged macrocycles have received special interest due to their potential stronger interactions with negatively charged tumor cell plasma membranes and bacterial surfaces, thus enhancing their cellular targeting ability.[10–13] Furthermore, cationic PS have been observed to localize subcellularly within the mitochondria,[14–18] lysosomes,[14,19,20] ER[16,17] and nuclei,[21] and to bind to anionic DNA and RNA,[22–25] which can enhance their overall PDT efficacy.

Herein we report the synthesis, spectroscopic properties and *in vitro* evaluation of a series of nine water-soluble ZnPcs containing one, two, four or eight trimethylaminophenoxy groups. We have recently observed significant differences in the cytotoxicity, cellular uptake and photodynamic ability of a series of porphyrins bearing similar cationic groups (−N−$(CH_3)_3^+$);[17] while all cationic porphyrins in this series targeted cell mitochondria, the most phototoxic was found to be the mono-cationic while the di-cationic accumulated the most within HEp2 cells. In another study[26] we observed that a Pc bearing a single quaternary ammonium group (−NH_3^+) was ~20-fold more phototoxic than its corresponding tetra-ammonium Pc toward HEp2 cells. We have also investigated the properties of a series of octa-cationic pyridyloxy-Pcs bearing different metal ions and axial ligands in human HEp2 cells.[20]

Results and discussion

Synthesis

The synthetic strategies to mono-, di-, tetra- and octa-cationic Pcs **4a, 4b, 6a, 6b, 8, 12, 14, 17a** and **17b** are shown in Schemes 1, 2 and 3. The three key precursors 3(4)-(p-*N*-Boc-aminophenoxy) phthalonitrile **2a,b** (Scheme 1) and 4, 5-di(p-*N*-Boc-aminophenoxy)phthalonitrile **10** (Scheme 2) were synthesized in >80% yields from commercially available 3(4)-nitrophthalonitrile or 4, 5-dichlorophthalonitrile and *p-N*-Boc-aminophenol in DMF at 80 °C, in the presence of potassium carbonate, following known methodologies.[27,28] The key precursor 2, 2′-bis(2, 3-dicyanophenoxy)biphenyl 15 (Scheme 3), was also synthesized in 66% yield according to a known procedure.[29] When unprotected *p-aminophenol* was used instead in these reactions, lower yields (60–70%) of the corresponding aminophthalonitriles were obtained. Single crystals of the four phthalonitriles suitable for X-ray analyses were grown from dichloromethane, and their molecular structures are shown in Fig. 1. In **2a**, the dicyanophenyl group is essentially orthogonal to the central phenyl group, forming a dihedral angle of 89.83(3)° with it. The CO_2N plane is tipped considerably less from the central ring, forming a dihedral angle of 28.47(6)° with it. The conformation of **2b** is similar, with the dicyanophenyl and central phenyl rings forming a dihedral angle of 86.23(4)°, but its CO_2N plane is nearly coplanar with the central phenyl, having dihedral angle 3(1)°. In **10**, the dicyanophenyl plane is approximately orthogonal to both phenyl rings connected to it through O, the dihedral angles being 79.22(2)° and 85.25(2)°. The tips of the two CO_2N planes out of the phenyl groups to which they are bonded are intermediate between those seen in **2a** and **2b**, a 14.7(1)° and 14.9(1)°, but they tip their carbonyl O in opposite directions, one toward the $Ph(CN)_2$ and the other away from it. In diphthalonitrile **15**, the central diphenyl group has a torsion angle of 74.5(4)° about the bond linking the two rings. The dicyanophenyl groups are tipped by similar amounts out of the phenyl groups to which they are bonded, forming a dihedral angles of 70.68(7) and

NIH-PA Author Manuscript

NIH-PA Author Manuscript

NIH-PA Author Manuscript

67.60(7)° with them. The dicyanophenyl groups are nearly antiparallel, forming a dihedral angle of 7.7(4)°, and the molecule has nearly C_2 symmetry.

In order to enhance the solubility of the target cationic ZnPcs and to facilitate purification, 4-*tert*-butylphthalonitrile (rather than unsubstituted phthalonitrile) was chosen to perform the statistical condensation[28–30] with the corresponding 3(4)-(*p*-*N*-Boc-aminophenoxy)phthalonitrile (Scheme 1). The 3- or 4-(*p*-*N*-Boc-aminophenoxy)phthalonitrile (**2a** or **2b**) was treated with 3 equiv. 4-*tert*-butylphthalonitrile in the presence of $Zn(_{II})$ acetate and a catalytic amount of 1, 5-diazabicyclo(4.3.0)non-5-ene (DBN) in dimethylaminoethanol (DMAE). After heating the reaction mixture at 140 °C for 5 h, a mixture of ZnPcs was obtained, containing the A4-type Pc as the major product, followed by the A_3B- and A_2B_2-types ZnPcs, as determined by TLC and MS analyses. Purification of the mixture by column chromatography using mixtures of hexane and ethyl acetate for elution, gave the corresponding Boc-protected A_3B-type ZnPcs in 15–20% yields and the A_2B_2-type ZnPcs in 19–25% yields. Subsequent deprotection of the Boc groups using TFA in dichloromethane at room temperature, gave ZnPcs 3 and 5 in >90% yield. Lower yields of target Pcs **3** and **5** were obtained when N-unprotected aminophthalonitriles were used in the tet-racyclization. The quaternization reaction of the free amino groups was accomplished with excess methyl iodide and diisopropylamine (DIPA) in DMF at room temperature,[17] and the corresponding trimethylaminophenoxy-substituted ZnPcs **4** and **6** were isolated in 50–70% yields. The A_3B- and A_2B_2-type ZnPcs **4** and **6** are mixtures of regioisomers.[30–34] In particular the di-cationic ZnPcs 6 are complex mixtures of about 15 regioisomers of both *trans*-ABAB and *cis*-AABB types, and their separation was not performed due to their extremely similar retention times on reversed-phase HPLC. It is likely that the distribution of isomers is slightly different for the α- and β-substituted Pcs, due to the higher steric hindrance caused by neighboring α-substituents during the macrocyclization step, as previously reported.[35] The reversed-phase HPLC chromatograms obtained for cationic ZnPcs **6a** and **6b** using water/methanol (50 : 50 → 0 : 100) (not shown) were consistent with the expected mixtures of regioisomers. With the aim to decrease the number of isomers, the adjacent-substituted Pcs **16** were synthesized as shown in Scheme 3. Diphthalonitrile **15**, linked *via* the *ortho*-positions of biphenyl, was synthesized as previously reported,[28] and used to prevent the formation of the *trans*-ABAB Pc species. This reduced the number of possible regioisomers in the cyclotetramerization reaction, from fifteen to only three.

Macrocyclization of 4-(*p*-*N*-Boc-aminophenoxy) phthalonitrile **2b** under similar conditions as described above, followed by deprotection with TFA, gave tetra-amino ZnPc **7** as a mixture of regioisomers, in 20% yield (Scheme 1). Quaternization using excess methyl iodide gave ZnPc **8** in 82% yield. Following similar methodologies, di-amino ZnPcs **11** and **16** were synthesized from 4, 5-di(*N*-Boc-phenoxyl)phthalonitrile **10** and 2, 2′-bis(2, 3-dicyanophenoxy)biphenyl **15**, respectively, as shown in Schemes 2 and 3. The A_3B-type ZnPc **11** was isolated in 9% yield after TFA deprotection, while Pcs **16** were isolated in 13% **(16a)** and 10% (**16b**) yields. The octa-amino ZnPc **13** was obtained in 50% yield from cyclotetramerization of phthalonitrile **10**. Quaternization of the amino groups of ZnPcs **11, 13** and **16** using a large excess of methyl iodide gave the corresponding cationic ZnPcs **12, 14** and **17** in 50–90% yields.

Spectroscopic and photophysical characterization

All cationic ZnPcs **4a, 4b, 6a, 6b, 8, 12, 14** and **17** are soluble in polar organic solvents, such as DMSO, DMF, THF and methanol. Interestingly, the solubility of these ZnPcs in organic solvents was observed to decrease with increasing cationic charge, while their water solubility increased with cationic charge **(4a ~ 4b ~ 6a ~ 12 ~ 17a ~ 17b < 6b < 8 < 14)**. This facilitated the isolation of the tetra- and octa-cationic ZnPcs **8** and **14** after

NIH-PA Author Manuscript

NIH-PA Author Manuscript

NIH-PA Author Manuscript

quaternization reaction in DMF and DIPA, since these ZnPcs readily precipitated from solution upon exhaustive methylation. Only Pcs **6b, 8** and **14** were water-soluble: Pc **14** at 2.69×10^{-3} M, Pc **8** at 4.75×10^{-3} M and **Pc 6b** at 4.03×10^{-3} M in distilled water. In addition, **Pc 14** was highly hygroscopic. All other Pcs formed aggregates in water, even upon sonication. However, all Pcs remained in aqueous solution when diluted from concentrated stocks in DMF or DMSO into PBS (final DMF or DMSO concentration of 1%) at 10 μM concentrations. MS analysis revealed that these ZnPcs can be readily N-demethylated; for example the mass spectrum on ZnPc **14** displays a large number of fragments, dominated by a peak at *m/z* 1671.679 $[M\text{-}8I\text{-}7CH_3]^+$. N-Demethylation of the cationic ZnPcs was also observed upon storage for over one week at room temperature, as previously observed.[36,37]

The complexity of the ^{1}H- and ^{13}C-NMR spectra of ZnPcs **4, 6**, and **8** suggests the presence of various regioisomers (up to fifteen for the di-cationic ZnPcs), as expected from the cyclo-tetramerization reaction of two mono-substituted phthalonitriles, and also consistent with our observations from reversed-phase HPLC. In the ^{1}H-NMR data of the N-Boc-protected Pc precursors, two sets of signals were observed for the *tert*-butyl protons on the macrocycle (centered at ~1.9 ppm) and the N-Boc group(s) (centered at ~1.5 ppm). Interestingly the α-substituted N-Boc Pc-precursors showed two sets of signals for the N-Boc group (centered at 1.4 and 1.5 ppm), while the β-substituted N-Boc Pc precursors showed only one set centered at 1.6 ppm. The same was observed for the N-Boc precursors of Pcs **16a,b**. Similarly, the mono- and di-cationic ZnPcs showed distinct differences in the chemical shifts of their $N(CH_3)_3$ protons, probably due to macrocycle distortion and/or hindered rotation. For example, while the β-substituted ZnPc **4b** shows only one singlet for the $N(CH_3)_3$ protons at 3.98 ppm, the α-substituted ZnPc **4a** shows two singlets at 3.62 and 3.72 ppm. Similarly the di-cationic β-substituted ZnPc **12** shows only one singlet for the $N(CH_3)_3$ protons at 3.96 ppm, while the di-cationic **6a** and **6b** both show several signals. Due to the ease of N-demethylation of the cationic ZnPcs, in particular under heat,[36, 37] their purification was conducted at room temperature (< 40 °C) and immediately followed by their NMR and MS characterization.

The spectroscopic properties of cationic ZnPcs **4a, 4b, 6a, 6b, 8, 12, 14, 17a** and **17b** in DMF and PBS at pH 7.4 are summarized in Tables 1 and S1 of the ESI,† respectively. All ZnPcs showed strong Q absorption bands between 680–686 nm and emissions between 682–689 nm in DMF. In PBS at pH 7.4 the ZnPcs showed broadened and less intense absorption bands, as well as fluorescence quenching, indicating aggregation (ESI, Fig. S1–S2, S10–S14†). The Stokes' shifts ranged between 2–4 nm in both DMF and PBS. Slight red shifts (1–5 nm) were observed in the absorption bands of the α- *versus* the β-substituted ZnPcs. No aggregation of the Pcs was observed at up to 8.8 μM concentrations in DMF. At this concentration, all the ZnPcs show a Soret absorption band between 330–370 nm, a strong Q band centered at ~684 nm and two vibrational bands at ~620 and 650 nm that strictly follow the Lambert-Beer law, characteristic of non-aggregated Pcs in DMF[38] (ESI, Fig. S1–S9†). At 1000 μM concentrations in DMF no colloidal solutions were observed for any of the ZnPcs, indicating that large aggregates were not formed.[39] All compounds exhibited fluorescence quantum yields in the range 0.11–0.21 in DMF, characteristic of this type of compound.[39–41] The singlet oxygen quantum yields were determined in DMF using ZnPc as the reference and 1.3-diphenylisobenzofuran (DPBF) as the scavenger of singlet oxygen.[42] The absorption decay of DPBF was monitored at 417 nm and used to calculate the singlet oxygen quantum yields, with an accuracy of ~10% (Table 1). The highest quantum yield

†Electronic supplementary information (ESI) available: Absorption and emission figures for all cationic ZnPcs in DMF and in PBS at pH = 7.4. CCDC reference numbers 810389 and 835347. For ESI and crystallographic data in CIF or other electronic format see DOI: 10.1039/c1md00232e

NIH-PA Author Manuscript

NIH-PA Author Manuscript

NIH-PA Author Manuscript

was found for the mono-cationic ZnPc **4a** (0.47) and the lowest for di-cationic ZnPc **12** (0.16). The observed range of singlet oxygen quantum yields suggests that this series of ZnPcs are efficient producers of singlet oxygen and therefore could be promising PDT photosensitizers.

Cellular studies

The *in vitro* biological properties of this series of cationic ZnPcs, including the time-dependent cellular uptake, cytotoxicity and intracellular localization, were investigated in human carcinoma HEp2 cells. The cytotoxicity was evaluated using the Promega's CellTiter Blue viability assay, as we have previously reported,[17] at concentrations up to 400 μM for each cationic ZnPc and for the octa-amino-Pc **13**. The results obtained are summarized in Table 2 (the IC_{50} values were calculated from dose-response curves). The cytotoxicity observed for this series of Pcs varied significantly and it depends not only on the number of charges but also on the Pc's substitution site, i.e. on α- *vs*. β-substitution. While we have previously reported high phototoxicity for a mono-cationic porphyrin bearing one $–N(CH_3)_3^+$ group[17] and a mono-cationic Pc with a $–NH_3^+$ group,[26] in this series of Pcs the most phototoxic were the di-cationic, and in particular the a-substituted Pcs. While all compounds show low dark cytotoxicity, with calculated IC_{50} > 150 μM, the ZnPcs bearing one and two positive charges were phototoxic toward HEp2 cells at 1.5 J cm^{-2} light dose. The most phototoxic were the di-cationic ZnPcs **6a ~ 17a** > **17b ~ 6b** > **12** with determined IC_{50} of 2.7, 2.7, 12.1, 13.4 and 39.6 μM, respectively, followed by mono-cationic ZnPc 4a with IC_{50} of 46.3 μM. All other Pcs show IC_{50} > 100 μM at 1.5 J cm^{-2}, including the mono-cationic **4b** and the octa-amino-Pc **13**. The phototoxicity observed for the ZnPcs does not directly correlate with the determined single oxygen quantum yields, because in addition to $^1O_2$ other ROS can be involved in the observed photo-induced cytotoxicity, and their site(s) of generation will also determine the mechanisms and efficacy of cell death. However, it is very interesting to note that the α--substituted Pcs (**4a, 6a** and **17a)** were significantly more phototoxic (*ca*. 5-fold enhancement) than their P-substituted analogs. Furthermore, there was no significant difference in the phototoxicity of the di-cationic **6a** and **17a**, nor of **6b** and **17b**, although Pcs **6a,b** are mixtures of about 15 regioisomers, containing both the cis-A_2B_2 and *trans-ABAB* macrocycles, whereas **17a,b** are mixtures of 3 regioisomers of only the *cis*-A_2B_2 type. These results suggest that the most phototoxic are the *cis*-A_2B_2 Pcs. In addition, Pc **6a** bearing the two positive charges on different (both adjacent and opposite) benzene rings was 15-fold more phototoxic than Pc **12** bearing the two positive charges on the same benzene ring, further indicating the significant effect of the α- *vs*. β-substitution on Pc phototoxicity. Among all the Pcs investigated, **6a** and **17a** were found to be the most phototoxic and to have the highest dark cytotoxicity/phototoxicity ratio of >120, and therefore the most promising for PDT applications.

Significant differences were also observed in the cellular uptake of this series of ZnPcs, as shown in Fig. 2. All ZnPcs showed similar uptake patterns with rapid accumulation at short times followed by a plateau reached 1–2 h after Pc exposure. The octa-amino-Pc **13** accumulated the most within cells, probably due to its higher hydrophobicity compared with the cationic ZnPcs. Among the cationic Pcs the di-cationic ZnPc **12** was observed to have the highest uptake values at all time points investigated, while the tetra-cationic Pc 8 had the lowest. These results indicate that the amphiphilicity of the cationic Pcs plays a crucial role on the extent of their cellular uptake, in agreement with previous reports;[17,26,43] in the porphyrin series, the di-cationic macrocycles were also found to accumulate the most within HEp2 cells. The two positive charges on the (β-positions of a single isoindole unit in ZnPc **12** confers higher amphiphilicity to the macrocycle, compared with the regioisomeric mixtures in **6a,b** and **17a,b**, which enhances hydrophobic/hydrophilic interactions that lead to increased cellular uptake.

NIH-PA Author Manuscript

NIH-PA Author Manuscript

NIH-PA Author Manuscript

The main sites of subcellular localization of the cationic Pcs were also investigated by fluorescence microscopy, upon exposure of HEp2 cells to 10 μM Pc for 6 h. Fig. 3–12 show the fluorescent patterns observed for each cationic ZnPc. Co-localization experiments were conducted using the organelle specific fluorescent probes ER Tracker Blue/White (endoplasmic reticulum, ER), MitoTracker Green (mitochondria), BODIPY Ceramide (golgi) and LysoSensor Green (lysosomes) to evaluate the main sites of subcellular localization. The di-cationic Pc **6a** was found mainly in mitochondria, and to a lower extent in the lysosomes and ER. Pc **17a** localized mainly in the ER and lysosomes, but not in mitochondria. On the other hand the tetra- and octa-cationic Pcs **8** and **14** were mainly found in mitochondria and to a lower extent in the Golgi, but not in the ER. The di-cationic ZnPcs **6b** and **12** localized mainly in the lysosomes and Golgi, respectively, and to a smaller extent in the ER. Pc 17b also localized mainly in the Golgi and ER. However, the monocationic ZnPcs **4a** and **4b** localized mainly in the lysosomes and Golgi, respectively, and were also observed in the ER. These results show very different subcellular distributions for this series of cationic ZnPcs, that might result from their different interactions with membranes and other biological substrates, and possibly different cellular uptake mechanisms. We have previously observed that a series of octa-cationic-Pcs localized intracellularly mainly in the lysosomes,[20] and that cationic porphyrins bearing up to four charges localized mainly in mitochondria, ER and/or lysosomes.[15–17] The high phototoxicity observed for ZnPcs **6a, 6b, 17a, 17b, 12** and **4a** might in part be due to their localization in the **ER**; some of these Pcs also localized in the mitochondria and/or the lysosomes, and all these organelles are important targets for PDT-induced cell apoptosis.[44–46] Interestingly, the octa-amino Pc **13** was mainly found in mitochondria and Golgi, and to a lower extent in lysosomes, but no localization was observed in the ER (Fig. 12), similar to cationic Pcs **8** and **14**.

Conclusions

The syntheses and properties of a series of nine cationic ZnPcs were investigated. All Pcs were prepared by a one-step cyclotetramerization of one or two phthalonitriles and consequently are mixtures of regioisomers, with exception of the octa-cationic and symmetrical ZnPc **14**. The positive charges conferred by the trimethylaminophenoxy groups and the presence of bulky *tert*-butyl groups in Pcs **4, 6** and **12** induced high solubility of these macrocycles in polar organic solvents. On the other hand, ZnPcs **17** were prepared using a biphenyl-linked diphthalonitrile and consequently consist of only the *cis*-A_2B_2 Pc regioisomers. The ZnPcs showed fluorescence quantum yields between 0.11 and 0.21 in DMF, and singlet oxygen quantum yields between 0.16 and 0.47 in the same solvent.

The cytotoxicity of this series of ZnPcs was found to depend both on the number of charges, and on their site of substitution (α *vs*. β) on the Pc isoindole units. On the other hand, the amphiphilic character of the molecules strongly determined their cellular uptake; the amphiphilic di-cationic ZnPc **12** was found to accumulate the most within cells, to have moderate phototoxicity (IC_{50} = 39.6 μM at 1.5 J cm^{-2}) and to localize preferentially in the Golgi apparatus. Among this series of Pcs, the di-cationic α-substituted ZnPcs **6a** and **17a** showed the highest phototoxicity (IC_{50} = 2.7 μM at 1.5 J cm^{-2}), partial localization in the ER, and highest ratio (>120) for dark cytotoxicity/phototoxicity, therefore are the most promising for PDT applications. The tetra- and octa-cationic Pcs showed very low cytotoxicities and localized mainly in cell mitochondria, suggesting possible application as mitochondria delivery vehicles for therapeutic agents.

NIH-PA Author Manuscript

NIH-PA Author Manuscript

NIH-PA Author Manuscript

Experimental section

Chemistry

All reagents and solvents were purchased from commercial sources and used directly without further purification. Silica gel 60 (230 × 400 mesh) and alumina neutral (activity I, 50–200 mm) from Sorbent Technologies were used for column chromatography. Sephadex G-100 and LH-20 were obtained from Amersham Biosciences. Analytical thin-layer chromatography (TLC) was carried out using polyester backed TLC plates 254 (pre-coated, 200 μm) from Sorbent Technologies. NMR spectra were recorded on an AV-400 LIQUID Bruker spectrometer (400 MHz for ^{1}H, 100 MHz for ^{13}C). Chemical shifts are reported in δ (ppm) using the following deuterated solvents as internal references: Acetone-d_6 2.05 ppm (^{1}H), 29.92 ppm (^{13}C); DMF-d_7 8.03 ppm (^{1}H), 163.15 ppm (^{13}C); Pyridine-d_5 7.58 ppm (^{1}H), 135.91 ppm (^{13}C); D_2O 4.80 ppm (^{1}H); THF-d_4, 3.58 ppm (^{1}H), 67.57 ppm (^{13}C); CD_2Cl_2 5.32 ppm (^{1}H), 54.00 ppm (^{13}C); $CDCl_3$ 7.27 ppm (^{1}H), 77.23 ppm (^{13}C). HPLC analyses were carried on a Dionex system equipped with a P680 pump and UVD340U detector. Electronic absorption spectra were measured on a PerkinElmer, Lambda 35 UV-Vis spectrometer and emission spectra were obtained on a Fluorolog® HORIBA JOBIN YVON (Model LFI-3751) spectrofluorimeter. MALDI-TOF mass spectra were recorded on a Bruker ProFlex III spectrometer using dithranol as the matrix; high-resolution ESI mass spectra were obtained on an Agilent Technologies 6210 Time-of-Flight LC/MS. Melting points were determined using MEL-TEMP electrothermal instrument.

Mono-*N*-Boc-amino-phthalonitrile (2a, 2b)—3-*N*-Boc-amino-phthalonitrile (**2a**): 3-nitrophthalonitrile (2 g, 11.6 mmol) and 4-*N*-Boc-aniline (3.6 g, 17.0 mmol) were dissolved in DMF (30 mL). Potassium carbonate (2.5 g, 18.0 mol) was added to the solution in five portions and the reaction solution was heated to 80 °C. After 3 h, the reaction solution was cooled to room temperature, poured into ice water and the solid was filtered. The crude product was purified by alumina column chromatography, eluted with dichloromethane to afford a white solid (3.1 g, 80.0%), mp 165–166 °C. ^{1}H NMR (acetone-d_6): δ 8.58 (br, 1H, NH), 7.80 (t, *J* = 8.2 Hz, 1H, Ar–H), 7.70–7.66 (m, 3H, Ar–H), 7.25–7.14 (m, 3H, Ar–H), 1.48 (s, 9H, $C(CH_3)_3$). ^{13}C NMR (acetone-d_6): δ 162.1, 153.7, 149.4, 138.6, 136.2, 128.1, 121.7, 121.5, 120.7, 117.4, 116.2, 113.8, 105.9 (Ar–C, CN), 80.2, 28.4 (C $(CH_3)_3$). HRMS-ESI: *m/z* 336.1340 $[M + H]^+$, calcd. for $[C_{19}H_{18}N_3O_3]^+$ 336.1342; 353.1604 $[M + H_2O]^+$, calcd. for $[C_{19}H_{19}N_3O_4]^+$ 353.1376; 358.1163 $[M + Na]^+$, calcd. for $[C_{19}H_{17}N_3O_3Na]^+$ 358.1168. For 4-*N*-Boc-amino-phthalonitrile (**2b**): A similar procedure as that described above for **2a** was followed and phthalonitrile **2b** was obtained in 87.8% yield, mp 169–171 °C. ^{1}H NMR (CD_2Cl_2): δ 7.73 (d, *J* = 8.7 Hz, 1H, Ar–H), 7.47 (d, *J* = 8.8 Hz, 2H, Ar–H), 7.27 (d, *J* = 2.3 Hz, 1H, Ar–H), 7.23 (dd, *J* = 8.6, 1H, Ar–H), 7.03 (d, *J* = 8.6, 2H, Ar–H), 6.72 (br, 1H, N–H), 1.51 (s, 9H, $C(CH_3)_3$). ^{13}C NMR ($CDCl_3$): δ 162.2, 152.6, 148.5, 136.8, 135.4, 121.3, 121.2, 121.1, 117.5, 115.6, 115.2, 108.6 (Ar–C, CN), 80.7 (C=O), 28.0 ($C(CH_3)_3$). MS (HRMS-ESI) *m/z* 336.1351 $[M + H]^+$, calcd for $C_{19}H_{18}N_3O_3$ 336.1348; 358.1189 $[M + Na]^+$, calcd for $C_{19}H_{17}N_3O_3Na$ 358.1162.

Mono-α-amino-ZnPc (3a)—A mixture of 4-*tert*-butylphthalonitrile (770.0 mg, 4.1 mmol), phthalonitrile **2a** (462.0 mg, 1.4 mmol) and zinc(II) acetate (509.4 mg, 2.8 mmol) was dissolved in DMAE (6.0 mL). Two drops of DBN were added and reaction solution refluxed for 5 h. The solvent was removed under vacuum and the residue was purified by column chromatography on silica gel using hexane/ethyl acetate 4 : 1 for elution. The N-Boc protected Pc was obtained as a blue solid (272 mg, 20.4%), mp > 250 °C. ^{1}H NMR (acetone-d_6): δ 9.51–8.07 (m, 11H, Ar–H), 7.78–7.23 (m, 5H, Ar–H), 1.86–1.82 (m, 27H, $C(CH_3)_3$), 1.51–1.48, 1.41 (m, 9H, $C(CH_3)_3$). ^{13}C NMR (acetone-d_6): δ 171.0 (C=O), 155.7, 155.0, 154.0, 153.9, 152.8, 151.9, 141.2, 139.3, 136.9, 135.6, 134.9, 134.8, 130.3, 127.7,

NIH-PA Author Manuscript

NIH-PA Author Manuscript

NIH-PA Author Manuscript

127.6, 127.3, 123.0, 122.4, 120.7, 120.5, 119.2, 119.0, 117.5, 117.5, 117.4, 117.3, 79.8, 79.7 (N–Boc–$C(CH_3)_3$), 60.6 (N–Ar–C), 36.5, 32.7, 32.5 (Ar–C, $C(CH_3)_3$), 28.7, 28.6 (N–Boc–$C(CH_3)_3$). MS (MALDI-TOF) *m/z* 952.389 $[M + H]^+$, calcd for $C_{55}H_{54}N_9O_3Zn$, 952.3641. This Pc was deprotected using dichloromethane/TFA 1 : 1 (8 mL), and **3a** was obtained as a blue solid (180 mg, 14.7% overall yield), mp > 250 °C. UV-Vis (DMF): λ_{max} (log ε) 349 nm (5.09), 614 nm (4.82), 682 nm (5.58). ^{1}H NMR (DMF-d_7): δ 9.58–9.29 (m, 7H, Ar–H), 8.41–8.28 (m, 4H, Ar–H), 7.28–7.24 (m, 2H, Ar–H), 6.69–6.63 (m, 2H, Ar–H), 4.65–5.05 (br, 2H, NH_2), 1.80– 1.65 (m, 27H, $C(CH_3)_3$). ^{13}C NMR (DMF-d_7): δ 156.6, 155.2, 155.0, 154.9, 154.8, 154.7, 154.6, 154.6, 154.1, 154.1, 153.9, 152.9, 150.1, 148.9, 145.7, 145.0, 142.1, 142.1, 139.8, 139.7, 139.4, 137.4, 137.3, 137.0, 131.5, 128.5, 128.4, 128.3, 127.5, 123.2, 123.0, 121.4, 119.7, 119.6, 119.4, 118.4, 117.6, 116.5, 116.4, 32.3 (Ar–C, C $(CH_3)_3$). MS (MALDI-TOF) *m/z* 852.341 $[M + H]^+$, calcd for $C_{50}H_{46}N_9OZn$ 852.312.

Mono-β-amino-ZnPc (3b)—A mixture of 4-*tert*-butylph-thalonitrile (385 mg, 2.09 mmol), phthalonitrile **2b** (231 mg, 0.69 mmol) and zinc(II) acetate (254.7 mg, 1.4 mmol) was reacted and purified as described above for Pc **3a** to afford a blue solid (121.6 mg, 18.5%), mp > 250 °C. ^{1}H NMR (acetone-d_6): δ 9.31–8.55 (m, 8H, Ar–H), 8.40–8.12 (m, 4H, Ar–H), 8.10–7.85 (m, 2H, Ar–H), 7.75–7.60 (m, 2H, Ar–H), 1.95–1.87 (m, 27H, $C(CH_3)_3$), 1.62 (d, J = 7.6, 9H, $C(CH_3)_3$). ^{13}C NMR (acetone-d_6): δ 159.9, 159.8, 159.3, 159.2, 154.1, 154.0, 153.7, 153.4, 153.0, 152.7, 152.4, 139.2, 138.9, 138.8, 138.7, 138.4, 138.2, 137.1, 137.0, 136.8, 136.7, 136.4, 136.2, 127.3, 125.9, 124.0, 123.8, 123.6, 122.9, 122.6, 122.4, 121.9, 121.5, 121.3, 121.0, 120.8, 120.7, 119.6, 119.2, 112.2, 111.4, 110.8 (Ar–C), 80.2 (N–Boc–$C(CH_3)_3$), 55.5 (N–A–C), 36.4, 32.6 (Ar–C, $C(CH_3)_3$), 28.9 (N–Boc–$C(CH_3)_3$). MS (MALDI-TOF) *m/z* 952.395 $[M + H]^+$, calcd for $C_{55}H_{54}N_9O_3Zn$ 952.364. The product was dissolved in dichloromethane/TFA 1 : 1 (8 mL) and the solution was stirred for 2 h to afford product **3b** (94.7 mg, 93.7%), mp > 250 °C. UV–Vis (DMF):λ_{max} (log ε) 349 nm (5.01), 610 nm (4.71), 677 nm (5.46). ^{1}H NMR (Pyridine-d_5): δ 10.02–9.70 (m, 6H, Ar–H), 9.63–9.41 (m, 1H, Ar–H), 8.44–7.96 (m, 4H, Ar–H), 7.47–7.39 (m, 2H, Ar–H), 7.18–7.10 (m, 2H, Ar–H), 5.09 (br, 2H, N–H), 1.72–1.65 (m, 27H, $C(CH_3)_3$). ^{13}CNMR (DMSO-d_6): δ 160.6, 160.6, 160.3, 160.3, 152.4, 152.2, 152.0, 151.9, 151.8, 151.7, 151.6, 151.4, 151.1, 147.2, 147.0, 146.5, 146.4, 146.2, 145.0, 143.9, 139.6, 139.5, 138.2, 138.0, 137.9, 137.7, 135.8, 135.7, 135.6, 135.5, 135.4, 131.9, 131.7, 131.2, 130.1, 126.9, 126.6, 125.1, 123.5, 122.8, 122.0, 121.8, 121.5, 121.4, 120.9, 120.7, 119.7, 118.7, 118.3, 115.9, 115.6, 115.0, 109.6, 109.4, 108.5, 108.3, (Ar–C), 59.8 (N–Ar–C), 35.6, 31.4 (Ar–C, $C(CH_3)_3$). MS (MALDI-TOF) *m/z* 852.348 $[M + H]^+$, calcd for $C_{50}H_{46}N_9OZn$ 852.312.

Mono-α-(trimethylamino)-ZnPc (4a)—Pc **3a** (20 mg, 0.023 mmol), DIPA (0.2 mL, 1.44 mmol) and CH_3I (0.5 mL, 8.0 mmol) were dissolved in dry DMF (0.3 mL) and the solution was stirred at room temperature for 3 days. Excess CH_3I was removed under reduced pressure. The mixture was dissolved in dichloromethane (15 mL) and washed with water (20 mL × 2). The organic layer was dried under vacuum and purified by gel permeation on Sephadex G-100 using dichloromethane/methanol 5:1 for elution. The title compound was obtained as a blue solid (18.2 mg, 75.8%), mp 204–206 °C. UV-Vis (DMF): λ_{max} (log ε) 351 nm (4.11), 620 nm (4.13), 684 nm (4.97). ^{1}H NMR (acetone-d_6): δ 9.47–9.16 (m, 6H, Ar–H), 8.85–7.82 (m, 8H, Ar–H), 7.50 (br, 2H, Ar–H), 3.72 (s, 4H, N–CH_3), 3.62 (s, 5H, N–CH_3), 1.80–1.71 (m, 27H, $C(CH_3)_3$). ^{13}CNMR (acetone-d_6): δ 162.2, 156.0, 153.9, 150.4, 142.8, 140.3, 137.9, 130.9, 128.0, 123.2, 123.0, 122.8, 122.6, 119.9, 118.2, 117.7 (Ar–C), 71.3 (N–Ar–C), 58.0, 57.9 (N–CH_3), 36.5, 32.6 ($C(CH_3)_3$). MS (MALDI-TOF) *m/z* 894.434 $[M – I]^+$, calcd for $C_{53}H_{52}N_9OZn$ 894.359.

Mono-β-(trimethylamino)-ZnPc (4b)—Pc **3b** (20 mg, 0.023 mmol), DIPA (0.2 mL, 1.44 mmol) and CH_3I (0.5 mL, 8.0 mmol) were dissolved in dry DMF (0.3 mL). Excess

NIH-PA Author Manuscript

NIH-PA Author Manuscript

NIH-PA Author Manuscript

CH_3I was removed under reduced pressure and the resulting residue purified as described above yielding a blue solid (15.7 mg, 65.4%), mp 201–203 °C UV-Vis (DMF): λ_{max} (log ε) 355 nm (4.22), 618 nm (3.90), 683 nm (4.80). ^{1}H NMR (DMF-d_7): δ 9.54–9.23 (m, 7H, Ar–H), 8.95 (br, 1H, Ar–H), 8.41–8.34 (m, 5H, Ar–H), 7.97–7.70 (m, 4H, Ar–H), 3.99 (s, 9H, N–3CH_3), 1.82–1.76 (m, 27H, C $(CH_3)_3$). ^{13}C NMR (DMF-d_7): δ 160.2, 159.4, 157.9, 155.32, 154.8, 154.2, 154.1, 153.9, 143.7, 141.3, 140.1, 139.9, 137.7, 137.5, 132.5, 128.3, 125.3, 124.0, 123.8, 123.3, 122.3, 120.7, 120.3, 119.9, 115.9, 113.8, 113.6 (Ar–C), 71.3 (N–Ar–C), 57.3 (N–CH_3), 32.6 (C$(CH_3)_3$). MS (MALDI-TOF) *m/z* 894.442 $[M - I]^+$, calcd for $C_{53}H_{52}N_9OZn$ 894.359.

Di-α-amino-ZnPc (5a)—The same procedure was followed as described above for Pc **3a**. Purification by column chromatography on silica gel using hexane/ethyl acetate 1 : 1 gave the N-Boc protected Pc as a blue solid (76 mg, 19.4% yield), mp > 250 °C ^{1}H NMR (DMF-d_7): δ 9.58–8.92 (m, 8H, Ar–H), 8.41–8.12 (m, 4H, Ar–H), 7.92–7.66 (m, 5H, Ar–H), 7.60–7.47 (m, 4H, Ar–H), 1.81–1.77 (m, 18H, C$(CH_3)_3$), 1.57, 1.51, 1.50, 1.46, 1.46, 1.42 (s, 18H, CH_3). ^{13}C NMR (acetone-d_6): δ 169.5, 169.2, (C=O), 155.9, 155.7, 155.3, 155.0, 154.9, 154.7, 154.6, 154.4, 154.2, 154.0, 153.9, 153.8, 153.7, 153.5, 153.5, 153.3, 153.0, 153.0, 152.9, 151.9, 151.6, 150.6, 142.0, 141.9, 141.4, 141.3, 141.0, 140.0, 139.9, 139.7, 139.5, 139.4, 139.2, 137.6, 137.3, 137.0, 136.7, 135.8, 135.6, 135.5, 135.0, 134.9, 130.4, 130.1, 129.7, 129.6, 129.2, 128.8, 128.6, 128.0, 127.6, 127.5, 127.3, 127.2, 123.7, 123.4, 123.3, 122.8, 122.7, 122.4, 122.1, 121.5, 121.3, 120.7, 120.1, 119.9, 119.4, 119.3, 119.1, 118.8, 118.4, 118.1, 117.6, 117.5, 117.4, 117.2 (Ar–C), 80.0, 79.8, 79.7 (*N*-Boc, C$(CH_3)_3$), 36.5, 36.4, 32.7, 32.5, 31.6, 31.4 (Ar–C, C $(CH_3)_3$), 28.9, 28.7, 28.6 (*N*-Boc, C$(CH_3)_3$). MS (MALDI-TOF) *m/z* 1102.455 $[M]^+$, calcd for $C_{62}H_{58}N_{10}O_6Zn$ 1102.383. The N-Boc protected Pc was dissolved in dichloromethane/TFA 1 : 1 (8 mL) and the solution was stirred for 2 h to afford Pc **5a** (163.1 mg, 93.1%), mp > 250 °C. UV-Vis (DMF): λ_{max} (log ε) 350 nm (4.55), 618 nm (4.31), 686 nm (5.07). ^{1}H NMR (DMF-d_7): δ 9.57–8.99 (m, 6H, Ar–H), 8.41–8.16 (m, 4H, Ar–H), 7.93–7.69 (m, 2H, Ar–H), 7.35 (br, 4H, Ar–H), 6.82 (br, 4H, Ar–H), 1.83–1.67 (m, 18H, C$(CH_3)_3$). ^{13}C NMR (DMF-d_7): δ 156.2, 156.1, 155.6, 155.3, 155.1, 155.0, 154.8, 154.6, 154.5, 154.4, 154.1, 153.9, 153.5, 153.3, 153.2, 152.4, 150.9, 143.3, 142.3, 141.6, 140.2, 140.0, 139.8, 137.8, 137.6, 137.4, 132.5, 131.8, 131.5, 129.9, 129.2, 128.7, 128.5, 128.1, 123.9, 123.4, 122.2, 121.3, 120.0, 119.6, 119.5, 118.5, 118.1, 118.1, 117.5 (Ar–C), 32.6 (Ar–C, C$(CH_3)_3$). MS (MALDI-TOF) *m/z* 903.352 $[M + H]^+$, calcd for $C_{52}H_{43}N_{10}O_2Zn$ 903.286.

Di-β-amino-ZnPc (5b)—The same procedure was followed as described above for Pc **3b**. Purification by column chromatography on silica gel using hexane/ethyl acetate 1 : 1 gave the N-Boc protected Pc as a blue solid (98.0 mg, 25% yield), mp 214–216 °C. ^{1}H NMR (DMF-d_7): δ 9.67–9.59 (m, 2H, Ar–H), 9.39–8.40 (m, 9H, Ar–H), 8.00–7.81 (m, 5H, Ar–H), 7.64–7.60 (m, 4H, Ar–H), 1.88–1.82 (m, 18H, C$(CH_3)_3$), 1.61–1.59 (m, 18H, N–Boc–C$(CH_3)_3$). ^{13}C NMR (DMF-d_7): δ 164.9, 161.1, 161.0, 160.7, 154.5, 154.3, 153.9, 153.8, 153.6, 153.4, 153.3, 153.0, 152.8, 150.5, 141.2, 139.8, 138.7, 138.0, 139.7, 137.4, 136.8, 134.1, 128.3, 127.6, 126.2, 124.8, 123.1, 122.2, 121.9, 121.8, 121.6, 121.5, 121.3, 121.1, 120.9, 119.8, 112.3, 111.4, 110.9, (Ar–C), 80.2 (C=O), 60.9 (N–Ar–C), 36.8, 32.7 (Ar–C, C$(CH_3)_3$), 29.0, 28.8 (N–Boc–C $(CH_3)_3$). MS (MALDI-TOF) *m/z* 1103.463 $[M + H]^+$, calcd for $C_{62}H_{59}N_{10}O_6Zn$ 1103.391. The N-Boc protected Pc was dissolved in dichloromethane/TFA 1 : 1 (8 mL) and the solution was stirred for 2 h to afford Pc **5b** (73.8, 92.0% yield), mp > 250 °C. UV–Vis (DMF): λ_{max} (log ε) 351 nm (4.90), 611 nm (4.59), 679 nm (5.32). ^{1}H NMR (DMSO-d_6):δ 9.40–8.82 (m, 9H, Ar–H), 8.56–8.18 (m, 5H, Ar–H), 7.87– 7.60 (m, 4H, Ar–H), 7.28–6.77 (m, 7H, Ar–H), 5.20–5.00 (br, 3H, N–H), 1.82–1.77 (m, 18H, C $(CH_3)_3$). ^{13}C NMR (DMSO-d_6): δ 160.7, 152.4, 152.2, 146.0, 139.6, 138.0, 135.4, 132.0, 131.8, 127.1, 123.8, 123.6, 121.5, 120.9, 118.8, 115.4, 114.9, 109.6, 108.3 (Ar–C), 35.6,

NIH-PA Author Manuscript

NIH-PA Author Manuscript

NIH-PA Author Manuscript

31.9, 31.5, 31.0, 30.7 (Ar–C, $C(CH_3)_3$). MS (MALDI-TOF) *m/z* 903.587 $[M + H]^+$, calcd for $C_{52}H_{43}N_{10}O_2Zn$ 903.286.

Di-α-(trimethylamino)-ZnPc (6a)—Pc **5a** (20 mg, 0.022 mmol), DIPA (0.15 mL, 1.07 mmol) and CH_3I (0.2 mL, 3.21 mmol) were dissolved in dry DMF (0.5 mL) and the solution was stirred at room temperature for 3 days. Excess CH_3I was removed under reduced pressure and the residue was purified using the same procedure as described above for Pc **4a**. Compound **6a** was obtained as a blue solid (16.2mg, 58.9% yield), mp 195–197 °C. UV-Vis (DMF): λ_{max} (log ε) 350 nm (4.64), 622 nm (3.79), 686 nm (5.25). ^{1}H NMR (acetone-d_6):δ 9.55–9.36 (m, 4H, Ar–H), 9.04–8.93 (m, 1H, Ar–H), 8.72–8.59 (m, 1H, Ar–H), 8.33–8.04 (m, 7H, Ar–H), 7.91– 7.75 (m, 2H, Ar–H), 7.66–7.54 (m, 4H, Ar– H), 3.85–3.65 (m, 18H, N–CH_3), 1.79–1.64 (m, 27H, $C(CH_3)_3$). ^{13}C NMR (acetone-d_6): δ 162.1, 161.7, 154.1, 153.7, 150.4, 143.0, 141.8, 140.5, 140.1, 138.1, 137.7, 132.1, 131.4, 130.3, 129.8, 128.2, 127.8, 123.8, 123.4, 123.0, 121.3, 119.8, 118.3, 117.7, (Ar–C), 66.3 (N–Ar–C), 57.9 (N–CH_3), 36.4, 32.7, 32.3 ($C(CH_3)_3$). MS (MALDI-TOF) *m/z* 973.373 $[M\text{-}2I\text{-}CH_3]^+$, calcd for $C_{57}H_{53}N_{10}O_2Zn$ 973.364.

Di-β-(trimethylamino)-ZnPc (6b)—Pc **5b** (20 mg, 0.022 mmol), DIPA (0.15 mL, 1.07 mmol) and CH_3I (0.2 mL, 3.21 mmol) were used to synthesize the title compound following the same procedure described above for Pc **6a**. Product **6b** was obtained as a blue solid (14.6 mg, 53.1% yield), mp > 218–220 °C. UV-Vis (DMF): λ_{max} (log ε) 355 nm (4.41), 618 nm (4.08), 683 nm (4.96). ^{1}H NMR (DMF-d_7): δ 9.60–9.9.06 (m, 9H, Ar–H), 8.36–8.24 (m, 6H, Ar–H), 7.66–7.57 (m, 4H, Ar–H), 7.40–7.37 (m, 1H, Ar–H), 7.05–7.02(m, 1H, Ar–H), 3.98–3.93 (m, 18H,N-6CH_3), 1.78–1.71 (m, 18H, $C(CH_3)_3$). ^{13}C NMR (DMF-d_7): δ 160.1, 158.1, 155.4, 154.0, 149.4, 143.7, 141.9, 140.4, 137.9, 136.4, 128.2, 125.3, 124.0, 123.1, 122.3, 122.1, 120.3, 119.9, 119.8, 115.1, 113.6, (Ar–C), 71.3 (N–Ar–C), 58.0 (N–CH_3), 41.5, 32.5 ($C(CH_3)_3$). MS (MALDI-TOF) *m/z* 973.654 $[M\text{-}2I\text{-}CH_3]^+$, calcd for $C_{57}H_{53}N_{10}O_2Zn$ 973.364.

Tetra-β-amino-ZnPc (7)—A mixture of phthalonitrile **2b** (0.5 g, 1.49 mmol) and zinc(II) acetate (0.095 g, 0.5 mmol) were added to DMAE (5.0 mL). The solution was heated under argon and two drops of DBN were added. The solution was refluxed for another 6 h. The solvent was removed and the product was purified by alumina column chromatography using dichloromethane/methanol 95 : 5 for elution. The product was further purified by a second alumina column using dichloromethane/methanol 9 : 1 for elution to afford a dark green solid (105.6 mg, 20.2%), mp > 250 °C. ^{1}H NMR (THF-d_4): δ 9.12–8.66 (m, 12H, Ar–H), 7.93–7.68 (m, 8H, Ar–H), 7.46–7.31 (br, 8H, Ar–H), 7.16 (br, 8H, Ar–H), 1.55 (s, 36H, $C(CH_3)_3$). ^{13}C NMR(THF-d_4): δ 160.9, 154.6, 154.1, 153.2, 152.8, 141.5, 137.6, 137.1, 134.4, 124.9, 121.2, 120.6, 112.1, 111.5 (Ar–C), 79.9 (N–Boc–$C(CH_3)_3$), 62.9, 59.1, 45.9 (N–Ar–C), 28.87 (*N*–Boc, $C(CH_3)_3$). MS (MALDI-TOF) *m/z* 1405.819 $[M + H]^+$, calcd for $C_{76}H_{69}N_{12}O_{12}Zn$ 1405.445. The solid was dissolved in dichloromethane/TFA 1 : 1 and the solution was stirred at 0 °C for 3 h. The solvent was removed under vacuum and the resulting residue was treated with 2 N NaOH (1 mL). The product was re-dissolved in 20 mL dichloromethane/ methanol and washed with water (2 × 50 mL). The organic phase was concentrated to afford a green solid (72.4 mg, 96.1%), mp > 250 °C UV-Vis (DMF): λ_{max} (log ε) 352 nm (4.63), 613 nm (4.31), 682 nm (5.01). ^{1}H NMR (DMF-d_7): δ 9.89 (br, 1H, Ar–H), 9.34–9.28 (m, 3H, Ar–H), 8.88–8.70 (m, 3H, Ar–H), 7.46–7.31 (m, 8H, Ar–H), 7.83 (br, 7H, Ar–H), 7.47 (br, 4H, Ar–H), 7.21 (br, 4H, Ar–H), 6.93 (br, 4H, Ar–H). ^{13}C NMR (DMF-d_7): δ 160.0, 159.5, 155.2, 154.0, 147.5, 142.0, 137.3, 135.4, 134.9, 134.3, 131.6, 124.8, 122.5, 121.2, 120.0, 116.5, 111.4, 110.1 (Ar–C), 63.4, 59.2, 154.5, 46.3 (N–Ar–C), 28.9 (*N*-Boc, $C(CH_3)_3$). MS (MALDI-TOF) *m/z* 1004.313 $[M + H]^+$, calcd for $C_{56}H_{36}N_{12}O_4Zn$ 1004.227.

NIH-PA Author Manuscript

NIH-PA Author Manuscript

NIH-PA Author Manuscript

Tetra-β-trimethylamino-ZnPc (8)—Pc **7** (24.4 mg, 0.023 mmol) was dissolved in DMF (0.4 mL). CH_3I (3 mL, 48.2 mmol) and DIPA (0.2 mL, 1.42 mmol) were added and the reaction mixture was stirred at room temperature for 3 days. Excess CH_3I was removed under reduced pressure. Acetone was added to triturate the product and the solution was centrifuged to yield the title compound as a blue-green solid (31.9 mg, 82.4%), mp 194–196 °C. UV-vis (DMF): λ_{max} (log ε) 358 nm (4.62), 620 nm (4.31), 684 nm (5.08). ^{1}H NMR (DMF-*d*$_7$): 9.49–9.32 (m, 2H, Ar–H), 9.00–8.89 (m, 2H, Ar–H), 8.34 (br, 5H, Ar– H), 7.85–7.75 (m, 7H, Ar–H), 7.71–7.64 (m, 7H, Ar–H), 7.53–7.47 (m, 6H, Ar–H), 4.07–4.01 (m, 36H, N–CH_3). ^{13}C NMR (DMSO-*d*$_6$): δ 158.2, 156.9, 153.1, 152.2, 151.8, 142.5, 142.3, 140.1, 139.9, 135.4, 134.9, 134.5, 133.5, 124.45, 124.3, 124.2, 123.0, 122.9, 122.7, 121.3, 121.1, 120.4, 120.1, 119.9, 119.5, 119.2, 119.1, 114.2, 112.8, 112.1 (Ar–C), 64.2 (N–Ar–C), 58.1, 56.8, 53.2 (N–CH_3). MS (MALDI-TOF) *m/z* 1131.406 $[M\text{-}4I\text{-}3CH_3]^+$, calcd for $C_{65}H_{55}N_{12}O_4Zn$ 1131.3761.

4,5-Di -*N*-Boc-amino-phthalonitrile (10)—The compound was synthesized from 4, 5-dichlorophthalonitrile and N-Boc-4-aniline in 82.6% yield, following the procedure described above for phthalonitrile **2a**; mp 203–205 °C. ^{1}H NMR ($CDCl_3$):δ 7.47 (d, *J* = 8.8 Hz, 4H, Ar–H), 7.15 (s, 2H, Ar–H), 7.05 (d, *J* = 8.8 Hz, 4H, Ar–H), 6.66 (br, 2H, N–H), 1.51 (s, 18H, 2 × $C(CH_3)_3$). ^{13}C NMR ($CDCl_3$): δ 152.8, 152.2, 148.9, 136.9, 136.5, 121.0, 120.9, 120.5, 115.6, 115.01, 110.0, 101.5 (Ar–C, CN), 81.0 (C=O), 28.3 ($C(CH_3)_3$). MS (ESI) *m/z* 565.2036 $[M + Na]^+$, calcd for $C_{30}H_{30}N_4O_6Na$ 565.2058.

Di-β-amino-ZnPc (11)—A mixture of 4-*tert*-butylphthalonitrile (385 mg, 2.09 mmol), phthalonitrile **10** (374 mg, 0.69 mmol) and zinc(II) acetate (254.7 mg, 1.4 mmol) was used and a similar procedure as described above for Pc **3a** was followed to afford a blue solid (81 mg, 10.1%), mp > 250 °C ^{1}H NMR (DMF-*d*$_7$): δ 9.56–9.24 (m, 7H, Ar–H), 9.12–9.02 (m, 1H, Ar–H), 8.91–8.83 (m, 2H, Ar–H), 8.42–8.31 (m, 3H, Ar–H), 7.89–7.79 (m, 4H, Ar–H), 7.52–7.40 (m, 4H, Ar–H), 1.85–1.79 (m, 27H, $C(CH_3)_3$), 1.58–1.53 (m, 18H, Boc-$C(CH_3)_3$). ^{13}CNMR (DMF-*d*$_7$): δ 154.5, 154.2, 154.0, 153.3, 152.7, 152.2, 151.6, 151.4, 151.1, 150.6, 150.4, 139.6, 137.5, 137.3, 137.0, 135.6, 135.2, 128.5, 123.2, 121.0, 120.6, 120.4, 120.3, 119.7, 119.5, 119.4, 119.2, 115.5, 113.7, 80.2(C=O), 80.0 (C=O), 32.6 (Ar–C, $C(CH_3)_3$), 29.9 ($C(CH_3)_3$), 28.9 (C $(CH_3)_3$). MS (MALDI-TOF) *m/z* 1158.465 $[M]^+$, calcd for $C_{66}H_{66}N_{10}O_6Zn$ 1158.446. The product was dissolved in dichloromethane/TFA 1 : 1 and the solution was stirred for 2 h to afford the title compound as a blue solid (61 mg, 9.2% overall yield), mp > 250 °C. UV-vis (DMF): λ_{max} (log ε) 353 nm (4.98), 611 nm (4.65), 677 nm (5.43). ^{1}H NMR (DMSO-*d*$_6$): δ 9.34–9.13 (m, 6H, Ar–H), 9.07–8.97 (m, 1H, Ar–H), 8.74–8.71 (m, 1H, Ar–H), 8.31–8.26 (m, 1H, Ar–H), 8.16–8.11 (m, 2H, Ar–H) 7.17–7.11 (m, 3H, Ar–H), 6.94–6.88 (m, 3H, Ar–H), 6.70–6.58 (br, 2H, Ar–H), 4.93 (br, 4H, N–H), 1.79–1.71 (m, 27H, $C(CH_3)_3$). ^{13}C NMR (DMSO-*d*$_6$): δ 152.9, 151.5, 147.1, 138.6, 136.2, 136.1, 133.8, 133.3, 127.6, 122.4, 121.1, 121.0, 120.1, 119.9, 118.8, 116.1, 115.8, 110.7, 32.3 (Ar–C, $C(CH_3)_3$). MS (MALDI-TOF) *m/z* 959.34 $[M + H]^+$, calcd for $C_{56}H_{51}N_{10}O_2Zn$ 959.35.

Di-β-trimethylamino-ZnPc (12)—Pc **11** (20 mg, 0.023 mmol), DIPA (0.2 mL, 1.44 mmol) and CH_3I (1.0 mL, 16.0 mmol) were dissolved in dry DMF (0.4 mL) and the solution was stirred at room temperature for 3 days. Excess CH_3I was removed under reduced pressure and the resulting residue was purified as described above for Pc **4a**. The title compound was obtained as a blue solid (19.5 mg, 72.0%), mp 190 °C (decomp). UV-vis (DMF): λmax (log ε) 357 nm (4.50), 619 nm (4.16), 684 nm (5.01). ^{1}H NMR (DMF-*d*$_7$): δ 9.56–9.23 (m, 9H, Ar–H), 8.45–8.28 (m, 7H, Ar–H), 7.60 (br, 3H, Ar–H), 3.96 (s, 18H, N-6CH_3), 1.78– 1.71 (m, 27H, $C(CH_3)$3). ^{13}C NMR (DMF-*d*$_7$): δ 159.8, 156.2, 155.5, 154.8, 154.1, 152.3, 149.0, 143.7, 140.3, 137.9, 137.1, 128.2, 123.9, 123.0, 119.8, 119.4,

NIH-PA Author Manuscript

NIH-PA Author Manuscript

NIH-PA Author Manuscript

119.1, 117.2, 116.3 (Ar–C), 71.3 (N–Ar–C), 58.0 (CH_3), 32.6 (C(CH_3)3). MS (MALDI-TOF) *m/z* 1029.416 $[M\text{-}2I\text{-}CH_3]^+$, calcd for $C_{61}H_{61}N_{10}O_2Zn$ 1029.427.

Octa-β-amino-ZnPc (13)—A mixture of phthalonitrile **10** (0.745 g, 1.37 mmol) and zinc(II) acetate (0.420 g, 2.29 mmol) were dissolved in DMAE (6.0 mL) under argon. Two drops of DBN were added and the solution was refluxed for 6 h. The solvent was removed and the residue was purified by column chromatography on Sephadex LH-20 using methanol for elution, to yield a green solid (462.0 mg, 59.0%), mp > 250 °C ^{1}H NMR (DMSO-d_6): δ 8.97 (s, 4H, Ar–H), 8.55 (s, 4H, Ar–H), 7.55 (s, 16H, Ar–H), 7.16 (s, 16H, Ar–H), 1.52 (s, 72H, C(CH_3)3). ^{13}C NMR (DMSO-d_6): δ 154.6, 154.0, 151.7, 136.9, 135.9, 120.4, 120.0, 119.5, 115.3, (Ar–C), 79.8 (C=O), 63.1, 62.9, 59.4, 59.3 (N–Ar–C), 46.1, 28.9 (*N*-Boc, C(CH_3)3). MS (MALDI-TOF) *m/z* 2277.901 $[M]^+$, $C_{123}H_{129}N_{16}O_{24}Zn$ 2277.866. The compound was dissolved in dichloromethane/TFA 1 : 1 and the solution was stirred for 2 h. The title product was obtained as a green solid (246.4 mg, 84.8%), mp > 250 °C. UV-vis (DMF): λ_{max} (log ε) 361 nm (4.62), 615 nm (4.22), 689 nm (5.06). $_1$H NMR (DMSO-d_6): δ 7.52 (br, 8H, Ar–H), 7.16–6.60 (m, 32H, Ar–H). ^{13}C NMR (DMSO-d_6): δ 153.6, 152.3, 145.7, 134.5, 120.0, 119.8, 115.2, (Ar–C), 61.7, 57.7, 53.1, 45.3 (N–Ar–C). MS (MALDI-TOF) *m/z* 1432.383 $[M]^+$, calcd for $C_{80}H_{56}N_{16}O_8Zn$ 1432.376.

Octa-β-trimethylamino-ZnPc (14)—Pc **13** (18.0 mg, 0.0126 mmol) was dissolved in DMF (8 mL). CH_3I (3 mL, 48.2 mmol) and DIPA (0.2 mL, 1.42 mmol) were added and the reaction mixture was stirred at room temperature for 3 days. Excess CH_3I was removed under reduced pressure. Acetone (5 mL) was added to triturate the product and the solution was centrifuged to yield the title compound as a green solid (31.9 mg, 90.9%), mp 188–190 °C UV-vis (DMF): λ_{max} (log ε) 365 nm (4.57), 620 nm (4.24), 686 nm (5.17). ^{1}H NMR (D_2O): δ 7.96–7.47 (m, 40H, Ar–H), 3.80–3.30 (m, 72H, N–CH3). ^{13}C NMR (D_2O): δ 158.1, 152.1, 142.0, 136.01, 134.8, 122.7, 120.1, 118.2, 117.6, 116.3, 114.4, (Ar–C), 64.1 (N–Ar–C), 62.6, 58.0, 56.7, 53.1, 42.2, 16.2 (N–CH3). MS (MALDI-TOF) *m/z* 1671.679 $[M\text{-}8I\text{-}7CH_3]^+$, calcd for $C_{97}H_{91}N_{16}O_8Zn$ 1671.650.

Di-a-amino-ZnPc (16a)—A mixture of 2, 2′-bis(2, 3-dicyanophenoxy)biphenyl **15**[29] (302.3 mg, 0.69 mmol), phthalonitrile **2a** (480.0 mg, 1.43 mmol) and zinc acetate (254.7 mg, 1.4 mmol) was dissolved in DMAE (5.0 mL). One drop of DBN was added and the solution was refluxed at for 5 h. After solvent removal under vacuum, the residue was purified by silica gel column chromatography using ethyl acetate. The product was further purified by a second silica column using hexane/ethyl acetate 1 : 1 for elution, affording a blue solid (112.2 mg, 13.9%), mp > 250 °C. ^{1}H NMR (DMF-d_7): δ 9.53–9.07 (m, 5H, Ar–H), 8.41–8.06 (m, 4H, Ar–H), 7.80–7.15 (m, 19H, Ar–H), 1.56–1.49 (m, 18H, C (CH_3)$_3$). ^{13}CNMR (DMF-d_7): δ 161169.6, 168.0 (C=O), 159.0, 156.3, 156.2, 156.1, 154.9, 154.7, 154.6, 154.5, 154.4, 154.3, 154.2, 154.1, 154.0, 153.8, 153.6, 153.4, 153.0, 152.5, 152.4, 151.0, 150.8, 138.7, 137.4, 137.1, 136.6, 136.3, 135.5, 133.2, 132.0, 131.6, 131.3, 131.0, 130.8, 130.6, 130.3, 129.9, 129.3, 129.0, 128.9, 128.2, 126.5, 126.3, 125.7, 124.7, 124.2, 122.3, 122.2, 122.1, 121, 6, 121.5, 121.3, 121.2, 121.0, 120.9, 120.8, 119.7, 119.6, 119.2, 118.2, 118.1, 117.5, 117.0, 116.4, 112.9 (Ar–C), 80.3, 80.1, 80.0 (O–C(CH_3)$_3$), 28.94, 28.86 (C(CH_3)$_3$). MS (MALDI-TOF) *m/z* 1173.440 $[M + H]^+$, calcd for $C_{66}H_4{}_9N_{10}O_8Zn$ 1173.303. The Boc-protected Pc (85.06 mg, 0.073 mmol) was dissolved in a 1 : 1 mixture of dichloromethane/ TFA (6 mL) and the solution was stirred at 0 °C for 3 h. After work-up as above, a blue-greenish solid was obtained (65.4 mg, 92.1%). UV-Vis (DMF): λ_{max} (log ε) 336 nm (4.37), 624 nm (4.13), 691 (4.89) nm. ^{1}H NMR (DMF-d_7): δ 9.41–6.27 (m, 28H, Ar–H), 4.12 (br, 4H, NH_2). ^{13}C NMR (DMF-d_7): δ 159.0, 155.2, 155.0, 154.1, 153.0, 152.3, 150.9, 148.5, 146.5, 146.2, 142.8, 140.4, 133.1, 131.0, 129.9, 129.6, 129.3, 127.9, 126.3, 122.2, 122.0,

NIH-PA Author Manuscript

NIH-PA Author Manuscript

NIH-PA Author Manuscript

121.8, 121.1, 117.9, 117.3, 116.6, 116.3, 112.9 (Ar–C). MS (MALDI-TOF) *m/z* 973.210 [M + H]$^+$, calcd for $C_{56}H_{33}N_{10}O_4Zn$, 973.1978.

Di- β -amino-ZnPc (16b)—A mixture of 2, 2′-bis(2, 3-dicyano-phenoxy)biphenyl **15**[29] (302.3 mg, 0.69 mmol), phthalonitrile **2b** (480.0 mg, 1.43 mmol) and zinc acetate (254.7 mg, 1.4 mmol) was dissolved in DMAE (100.0 mL). Two drops of DBN were added and the reaction mixture was refluxed for 15 h. Reaction work-up and purification as described above for **16a** gave Boc-protected Pc as a blue solid (94.6 mg, 11.4%), mp > 250 °C. ^{1}H NMR (DMF-d_7): δ 9.59–9.54 (m, 2H, Ar–H), 9.26–9.06 (m, 2H, Ar–H), 8.67–8.26 (m, 3H, Ar–H), 810–8.05 (m, 1H, Ar–H), 7.98–7.14 (m, 19H, Ar–H), 1.59–1.51 (m, 18H, $C(CH_3)_3$). ^{13}CNMR (DMF-d_7): δ 169.6, 168.0 (C=O), 161.3, 161.2, 161.14, 161.06, 159.11, 159.07, 154.9, 154.5, 154.3, 154.0, 153.6, 153.1, 152.9, 152.8, 152.5, 151.6, 150.8, 15.7, 142.7, 142.4, 141.2, 137.9, 137.8, 137.4, 136.4, 133.6, 133.2, 131.3, 131.2, 130.8, 130.7, 130.3, 129.9, 129.4, 126.3, 126.2, 125.7, 125.0, 124.9, 124.8, 122.1, 121.7, 121.5, 121.3, 121.1, 120.9, 118.2, 112.9, 111.9 (Ar–C), 80.2 (O–$C(CH_3)_3$), 28.9, 28.8 ($C(CH_3)_3$). MS (MALDI-TOF) *m/z* 1173.419 [M + H]$^+$, calcd for $C_{66}H4_8N_{10}O_8Zn$ 1173.303. The Boc-protected Pc (51.6 mg, 0.044 mmol) was dissolved in a 1 : 1 mixture of dichloromethane and TFA (6 mL) and the solution was stirred at 0 °C for 3 h. After workup as above a blue-greenish solid of the title Pc was obtained (38.2 mg, 89.2%). UV-Vis (DMF): λ_{max} (log) 350 nm (4.29), 616 nm (3.99), 684 (4.72) nm. ^{1}H NMR (DMF-d_7): 9.84–6.34 (m, 28H, Ar–H), 4.30 (br, 4H, NH_2). ^{13}C NMR (DMF-d_7): δ 159.1, 156.2, 155.0, 154.3, 153.0, 150.9, 150.6, 148.8, 143.0, 142.2, 140.4, 134.2, 133.2, 131.2, 131.0, 130.9, 129.9, 129.6, 129.3, 126.2, 125.7, 125.4, 122.2, 122.0, 121.2, 116.9, 112.8, 109.8h (Ar–C). MS (MALDI-TOF) *m/z* 973.228 [M + H]$^+$, calcd for $C_{56}H_{33}N_{10}O_4Zn$, 973.1978.

Di-α-(trimethylamino)-ZnPc (17a)—Pc **16a** (20 mg, 0.021 mmol), DIPA (0.15 mL, 1.07 mmol) and CH_3I (0.2 mL, 3.21 mmol) were dissolved in dry THF (0.5 mL) and this solution was stirred at room temperature for 3 days. Reaction work-up as above gave Pc **17a** as a pale-green solid (14.7 mg, 53.3%), mp > 250 °C UV-Vis (DMF): λ_{max} (log ε) 337 nm (4.61), 613 nm (4.51), 685 nm (5.26). ^{1}H NMR (DMF-d_7): δ 9.52–9.36 (m, 3H, Ar–H), 8.79–8.63 (m, 1H, Ar–H), 8.44–8.36 (m, 2H, Ar–H), 8.30–8.18 (m, 6H, Ar–H), 8.10–7.95 (m, 2H, Ar–H), 7.78–7.72 (m, 5H, Ar–H), 7.58–7.55 (m, 2H, Ar–H), 7.33–7.06 (m, 7H, Ar–H), 3.95 (s, 8H, N–CH_3), 3.85–3.81 (m, 10H, N–CH_3). ^{13}C NMR (DMF-d_7): δ 161.5, 160.0, 159.0, 154.5, 154.3, 153.8, 153.5, 153.2, 152.7, 151.0, 150.7 143.9, 143.2, 143.1, 142.7, 133.2, 132.4, 131.8, 131.2, 129.9, 129.3, 126.7, 126.5, 126.2, 124.2, 124.0, 123.6, 123.4, 122.1, 121.9 121.4, 121.0, 119.7, 118.5, 118.3, 112.9 (Ar–C), 66.29 (N–Ar–C), 58.1, 58.0 (N–CH_3). MS (MALDI-TOF) *m/z* 1045.304 [M-2I–CH_3 + 2H]$^+$, calcd for $C_{61}H_{45}N_{10}O_4Zn^+$ 1045.2917.

Di-β-(trimethylamino)-ZnPc (17b)—Pc **16b** (20 mg, 0.021 mmol), DIPA (0.15 mL, 1.07 mmol) and CH_3I (0.2 mL, 3.21 mmol) were dissolved in dry THF (0.5 mL) and this solution stirred at room temperature for 3 days. Work-up as above gave Pc **17b** as a blue-green solid (16.1 mg, 58.3%), mp > 250 °C. UV-Vis (DMF): λ_{max} (log ε) 350 nm (4.72), 613 nm (4.48), 680 nm (5.23). ^{1}H NMR (DMF-d_7): δ 9.27–8.66 (m, 3H, Ar–H), 8.37–8.30 (m, 5H, Ar–H), 8.15– 8.06 (m, 1H, Ar–H), 7.91–7.55 (m, 9H, Ar–H), 7.41– 7.25 (m, 7H, Ar–H), 4.02–3.97 (m, 18H, N–CH_3). ^{13}CNMR (DMF-d_7): δ 159.9, 158.9, 158.4, 158.2, 154.4, 154.0, 153.6, 150.8, 143.9, 143.8, 141.8, 141.4, 136.2, 135.9, 135.6, 133.3, 131.6, 131.3, 131.0, 130.0, 129.3, 126.2, 125.3, 124.1, 122.5, 122.1, 121.1, 120.6, 120.2, 114.2, 113.8, 113.0 (Ar–C), 66.29 (N–Ar–C), 58.1 (N–CH_3). MS (MALDI-TOF) *m/z* 1312.435 [M]$^+$, 1029.296 [M-2I-2CH_3 + H]$^+$, calcd for $C_{62}H_{46}N_{10}I_2O_4Zn^+$ 1312.1084, $C_{60}H_{41}N_{10}O_4Zn^+$ 1029.2604.

NIH-PA Author Manuscript

NIH-PA Author Manuscript

NIH-PA Author Manuscript

Molecular structures

Crystal structure analyses of phthalonitriles **2a, 2b, 10** and **15** were based on data collected at T = 90 K on either a Nonius KappaCCD diffractometer equipped with Mo-Kα radiation (compound **2a**) or a Bruker Kappa Apex-II CCD diffractometer with Cu-Kα radiation (compounds **2b, 10** and **15**). The crystals were obtained by slow evaporation of mixed solvents dichloromethane/hexanes 5:1. The crystal structure analyses of these phthalonitriles confirm their successful syntheses. Crystal data: **2a**, $C_{19}H_{17}N_3O_3$, M_r = 335.36, monoclinic space group $P2_1/c$, a = 16.266(4), b = 11.114(3), c = 9.8401(16) Å, β = 101.629(13)°, V= 1742.4(7) Å^3, Z = 4, D_c = 1.278 Mg m^{-3}, θ_{max} = 30.0°, R = 0.047 for 5047 data and 232 refined parameters, CCDC 810389; **2b**, $C_{19}H_{17}N_3O_3$, M_r = 335.36, orthorhombic space group $Pca2_1$, a = 10.139(2), b = 8.597(2), c = 20.157(5) Å, V= 1757.0(7) Å^3, Z = 4, D_c = 1.268 Mg m^{-3},θ_{max} = 68.1°, R = 0.032 for 2507 data and 233 refined parameters, CCDC 810390;† **10**, $C_{30}H_{30}N_4O_6$, M_r = 542.58, triclinic space group $P\bar{1}$, a = 10.0348(5), b = 12.0728(6), c = 13.3158(10) Å, α = 110.460(5), β = 102.622(4), γ = 101.132(4)°, V= 1409.38(15) Å^3, Z= 2, D_c = 1.279 Mgm^{-3}, θmax = 68.6°, R = 0.037 for 4972 data and 373 refined parameters, CCDC 810391.**15**, $C_{28}H_{14}N_4O2$. 2.4(CH_2Cl_2), M_r = 642.25, triclinic space group P$\bar{1}$, a = 8.9371(4), b = 10.3208(5), c = 16.1899(7) Å, α= 77.863(2), β = 81.983(2), γ = 78.622(2)°, V = 1423.75(11) Å^3, Z = 2, D_c = 1.498 Mg mr^{-3},θ_{max} = 69.4°, R = 0.066 for 5068 data and 334 refined parameters, CCDC 835347.†

Spectroscopic studies

All absorption spectra were measured on a PerkinElmer, Lambda 35 UV-Vis spectrometer. All solvents used were HPLC grade. Stock solutions of 0.1–1 mM of all ZnPcs in DMF were prepared and subsequent dilutions were prepared by spiking 20– 250 mL of the corresponding stock solution into 10 or 18 mL of each solvent. Emission spectra were obtained on a Fluorolog®-HORIBA JOBIN YVON (Model LFI-3751) spectrofluorimeter. The optical densities of the solutions used for emission studies ranged between 0.04–0.05 at excitation wavelengths. All experiments were carried out within 2 h of solution preparation at room temperature (23–25 °C), using a 10 mm path length spectrophotometric cell. The fluorescent quantum yields (Φ_f) were determined in DMF solvent using a secondary standard method,[32] and compared with ZnPc (Φ_f = 0.17) used as reference [39,40,47] The singlet oxygen quantum yields (Φ_Δ) were determined in DMF solvent using a relative method,[42] and compared with ZnPc (Φ_f = 0.56) used as reference and DPBF as a scavenger. The samples were prepared in the dark and the concentration of DPBF was lowered to ~3.0 × 10^{-5} mol l^{-1} to avoid chain reactions. The absorption decay of DPBF was monitored at 417 nm and used to calculate the singlet oxygen quantum yields, with an accuracy of ~10%. All measurements were carried out at 23–25 °C.

Cell studies

Human carcinoma HEp2 cells were maintained in a 50 : 50 mixture of DMEM:AMEM (Invitrogen) supplemented with 5% FBS (Invitrogen), Primocin antibiotic (Invitrogen) and 5% CO_2 at 37 °C. The cells were subcultured twice weekly to maintain subconfluent stocks. The 4th to 15th passage cells were used for all the experiments.

Time-dependent cellular uptake—The HEp2 cells were plated at 7500 cells per well in a Costar 96-well plate and allowed to grow for 48 h. The Pc stock solutions were prepared at 32 μM in DMSO and diluted to give 20 μM in medium (a 2X stock). This was further diluted into the cells of the 96-well plate to make a final concentration of 10 μM with a maximum DMSO concentration of 1%. Uptake was allowed to continue for 0, 1, 2, 4, 8, 12 and 24 h. The uptake was terminated by removing the loading medium and washing the wells with PBS. The concentration of the compounds was measured from standard curves

NIH-PA Author Manuscript

NIH-PA Author Manuscript

NIH-PA Author Manuscript

using intrinsic fluorescence as measured with a BMG FLUOstar plate reader equipped with a 355 nm excitation and a 650 nm emission filter, as we have previously described.[17] The cells were measured using a CyQuant cell proliferation assay (Invitrogen) as per manufactures instruction, and the uptake was expressed in terms of nM compound per cell.

Dark cytotoxicity—The HEp2 cells were plated as described above for the uptake experiment. The compounds were diluted into medium to give a 400 μM concentration. Two-fold serial dilutions were then prepared to 50 μM, and the cells were incubated overnight. Cell toxicity was measured using Promega's Cell Titer-Blue Viability assay as per manufacturer's instructions, with untreated cells considered 100% viable and cells treated with 0.2% saponin as 0% viable. The IC_{50} values were determined from dose-response curves obtained using GraphPad Prism software.

Phototoxicity—The cells were prepared as described above with compounds concentration range from 6.25–100 μM. After loading overnight, the medium was replaced with medium containing 50 μM HEPES pH 7.2. The cells were exposed to a NewPort light system with 175 W halogen lamp for 20 min, filtered through a water filter to provide approximately 1.5 J cm^{-2} light dose. The cells were kept cool by placing the culture on a 5 °C Echotherm chilling/heating plate (Torrey Pines Scientific, Inc.). After exposure to light, the plate was incubated overnight. Cells viability was then measured as described above for the dark cytotoxicity.

Microscopy—The cells were incubated in the glass bottom 6-well plate (MatTek) and allowed to grow for 48 h. The cells were then exposed to 10 μM of each compound overnight. Organelle tracers were obtained from Invitrogen and used at the following concentrations: LysoSensor Green 50 nM, MitoTracker Green 250 nM, ER Tracker Blue/white 100 nM, and BODIPY FL C5 ceramide 1 μM. The organelle tracers were diluted in medium and the cells were incubated concurrently with porphyrin and tracers for 30 min before washing 3 times with PBS and microscopy. Images were acquired using a Leica DMRXA microscope with 40 × NA 0.8dip objective lens and DAPI, GFP and Texas Red filter cubes (Chroma Technologies).

Supplementary Material

Refer to Web version on PubMed Central for supplementary material.

Acknowledgments

The work described was supported by the National Institutes of Health, grant number R21 CA139385.

Notes and references

1. Dougherty TJ, Gomer CJ, Henderson BW, Jori G, Kessel D, Korbelik M, Moan J, Peng Q. J. Natl. Cancer Inst. 1998; 90:889–905. [PubMed: 9637138]
2. Hahn SM, Glatstein E. Rev. Contemp. Pharmacother. 1999; 10:69–74.
3. Pandey RK. J. Porphyrins Phthalocyanines. 2000; 4:368–373.
4. Huang Z. Technology in Cancer Research & Treatment. 2005; 4:283–293. [PubMed: 15896084]
5. Brown SB, Brown EA, Walker I. Lancet Oncol. 2004; 5:497–508. [PubMed: 15288239]
6. Josefsen LB, Boyle RW. Met.-Based Drugs. 2008:1–24.
7. Ali H, van Lier JE. Chem. Rev. 1999; 99:2379–2450. [PubMed: 11749485]
8. Allen CM, Sharman WM, van Lier JE. J. Porphyrins Phthalocyanines. 2001; 5:161–169.
9. Ben-Hur, E.; Chan, W-S. The Porphyrin Handbook. Kadish, KM.; Smith, KM.; Guilard, R., editors. Vol. 19. Boston: Academic Press; 2003. p. 1-35.

NIH-PA Author Manuscript NIH-PA Author Manuscript NIH-PA Author Manuscript

10. Wohrle D, Iskander N, Graschew G, Sinn H, Friedrich EA, Maierborst W, Stern J, Schlag P. Photochem. Photobiol. 1990; 51:351–356. [PubMed: 2356230]
11. Reddi E, Ceccon M, Valduga G, Jori G, Bommer JC, Elisei F, Latterini L, Mazzucato U. Photochem. Photobiol. 2002; 75:462–470. [PubMed: 12017471]
12. Sol V, Branland P, Chaleix V, Granet R, Guilloton M, Lamarche F, Verneuil B, Krausz P. Bioorg Med. Chem. Lett. 2004; 14:4207–4211. [PubMed: 15261271]
13. Minnock A, Vernon DI, Schofield J, Griffiths J, Parish JH, Brown SB. J Photobiol Photochem B. 1996; 32:159–164.
14. Dummin H, Cernay T, Zimmermann HW. J Photobiol Photochem B. 1997; 37:219–229.
15. Kessel D, Luguya R, Vicente MGH. Photochem. Photobiol. 2003; 78:431–435. [PubMed: 14653572]
16. Sibrian-Vazquez M, Nesterova IV, Jensen TJ, Vicente MGH. Bioconjugate Chem. 2008; 19:705–713.
17. Jensen TJ, Vicente MGH, Luguya R, Norton J, Fronczek FR, Smith KM. J Photobiol Photochem B. 2010; 100:100–111.
18. Duan WB, Lo PC, Duan L, Fong WP, Ng DKP. Bioorg. Med. Chem. 2010; 18:2672–2677. [PubMed: 20223676]
19. Ricchelli F, Franchi L, Miotto G, Borsetto L, Gobbo S, Nikolov P, Bommer JC, Reddi E. Int. J. Biochem. Cell Biol. 2005; 37:306–319. [PubMed: 15474977]
20. Li H, Fronczek FR, Vicente MGH. J. Med. Chem. 2008; 51:502–511. [PubMed: 18189349]
21. Villanueva A. J Photobiol Photochem B. 1993; 18:295–298.
22. McMillin DR, Shelton AH, Bejune SA, Fanwick PE, Wall RK. Coord. Chem. Rev. 2005; 249:1451–1459.
23. Caminos DA, Durantini EN. J Photobiol Photochem A. 2008; 198:274–281.
24. Fu BQ, Zhang D, Weng XC, Zhang M, Ma H, Ma YZ, Zhou X. Chem.-Eur. J. 2008; 14:9431–9441. [PubMed: 18752229]
25. Chen B, Wu S, Li AX, Liang F, Zhou X, Cao XP, He ZK. Tetrahedron. 2006; 62:5487–5497.
26. Sibrian-Vazquez M, Ortiz J, Nesterova IV, Fernandez-Lazaro F, Sastre-Santos A, Soper SA, Vicente MGH. Bioconjugate Chem. 2007; 18:410–420.
27. Wohrle D, Eskes M, Shigehara K, Yamada A. Synthesis. 1993:194–196.
28. Sharman, WM.; van Lier, JE. The Porphyrin Handbook. Kadish, KM.; Smith, KM.; Guilard, R., editors. Vol. 15. Boston: Academic Press; 2003. p. 1-60.
29. Kobayashi N, Miwa H, Isago H, Tomura T. Inorg Chem. 1999; 38:479–485. [PubMed: 11673952]
30. Rodriguez-Morgade, MS.; de la Torre, G.; Torres, T. The Porphyrin Handbook. Kadish, KM.; Smith, KM.; Guilard, R., editors. Vol. 15. Boston: Academic Press; 2003. p. 125-160.
31. Giuntini F, Nistri D, Chiti G, Fantetti L, Jori G, Roncucci G. Tetrahedron Lett. 2003; 44:515–517.
32. Brykina GD, Uvarova MI, Koval YN, Shpigun OA. J. Anal. Chem. 2001; 56:940–944.
33. Uvarova MI, Brykina GD, Shpigun OA. J. Anal. Chem. 2000; 55:910–925.
34. Wang J, Liu H, Xue JP, Jiang Z, Chen NS, Huang JL. Chin. Sci. Bull. 2008; 53:1657–1664.
35. Rager C, Schmid G, Hanack M. Chem.-Eur. J. 1999; 5:280–288.
36. Filippis MP, Dei D, Fantetti L, Roncucci G. Tetrahedron Lett. 2000; 41:9143–9147.
37. Easson MW, Fronczek FR, Jensen TJ, Vicente MGH. Bioorg. Med. Chem. 2008; 16:3191–3208. [PubMed: 18178445]
38. Hofman J-W, van Zeeland F, Turker S, Talsma H, Lambrechts SAG, Sakharov DV, Hennink WE, van Nostrum CF. J. Med. Chem. 2007; 50:1485–1494. [PubMed: 17348640]
39. Zorlu Y, Dumoulin F, Durmus M, Ahsen V. Tetrahedron. 2010; 66:3248–3258.
40. Saka ET, Durmus M, Kantekin H. J. Organomet. Chem. 2011; 696:913–924.
41. Masilela N, Nyokong T. J. Lumin. 2010; 130:1787–1793.
42. Maree MD, Kuznetsova N, Nyokong T. J Photochem. Photobiol. A. 2001; 140:117–125.
43. Engelmann FM, Mayer I, Gabrielli DS, Toma HE, Kowaltowski AJ, Araki K, Baptista MS. J. Bioenerg. Biomembr. 2007; 39:175–185. [PubMed: 17436065]

NIH-PA Author Manuscript

NIH-PA Author Manuscript

NIH-PA Author Manuscript

44. Luo Y, Chang CK, Kessel D. Photochem. Photobiol. 1996; 63:528–534. [PubMed: 8934765]
45. Rao RV, Hermel E, Castro-Obregon S, del Rio G, Ellerby LM, Ellerby HM, Bredesen DE. J. Biol. Chem. 2001; 276:33869–33874. [PubMed: 11448953]
46. Kessel D. J. Porphyrins Phthalocyanines. 2004; 8:1009–1014.
47. Fery-Forgues S, Lavabre D. J. Chem. Educ. 1999; 76:1260–1264.

NIH-PA Author Manuscript
NIH-PA Author Manuscript
NIH-PA Author Manuscript

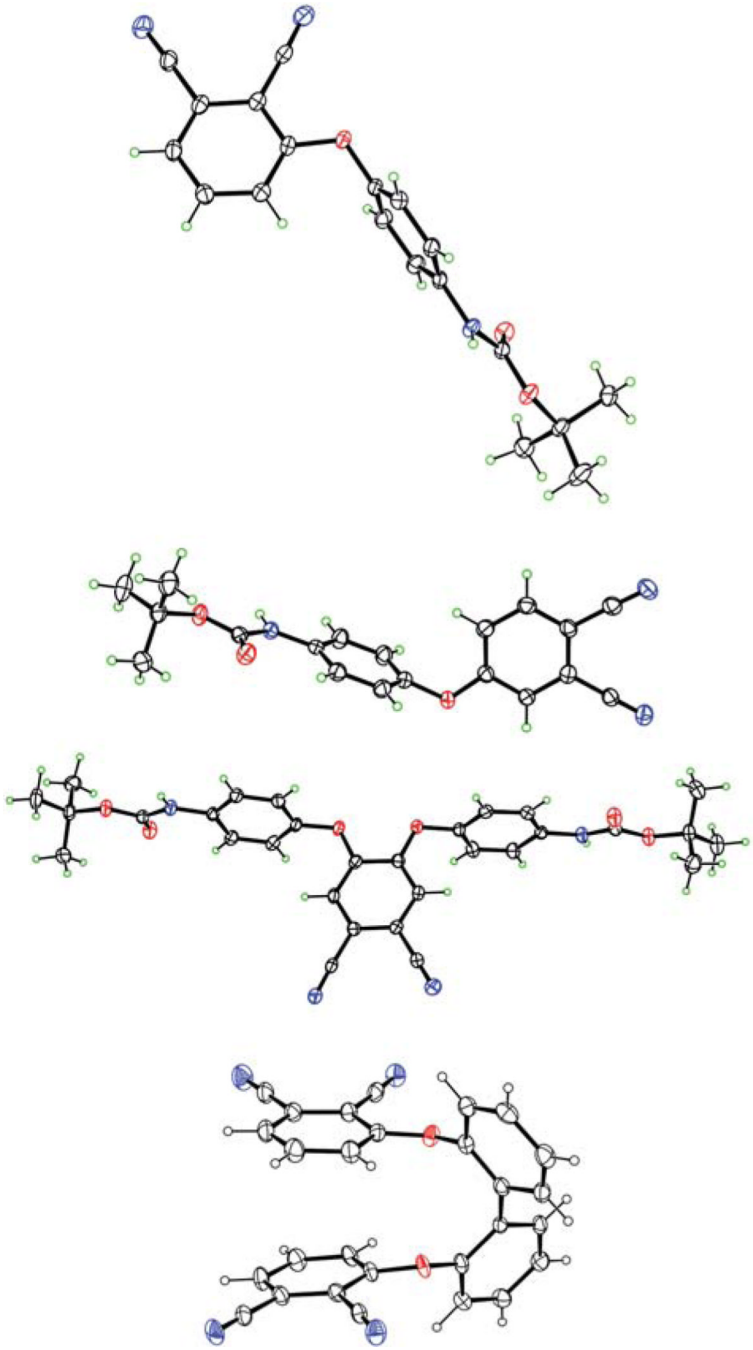

Fig. 1.
Molecular structures of phthalonitriles (from top) **2a, 2b, 10** and **15** from crystal structure determinations (N atoms are blue, O atoms red and H atoms green). Ellipsoids are drawn at the 50% probability level.

NIH-PA Author Manuscript
NIH-PA Author Manuscript
NIH-PA Author Manuscript

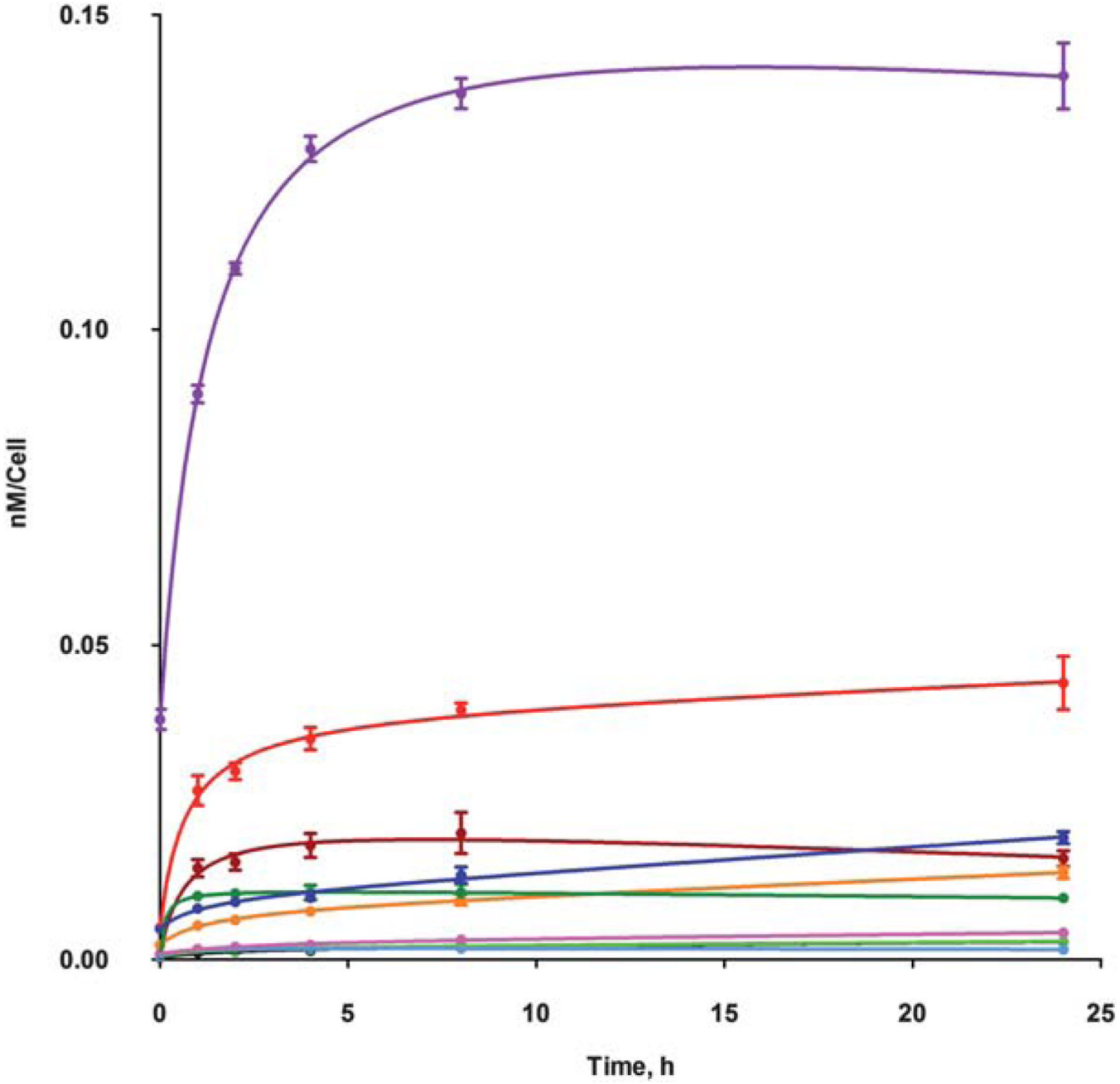

Fig. 2.

Time-dependent uptake of cationic ZnPcs at 10 μM by HEp2 cells: Pc **4a** (black), **4b** (brown), **6a** (orange), **6b** (green), **8** (light-blue), **12** (red), **13** (purple), **14** (dark-green), **17a** (blue) and **17b** (pink).

NIH-PA Author Manuscript
NIH-PA Author Manuscript
NIH-PA Author Manuscript

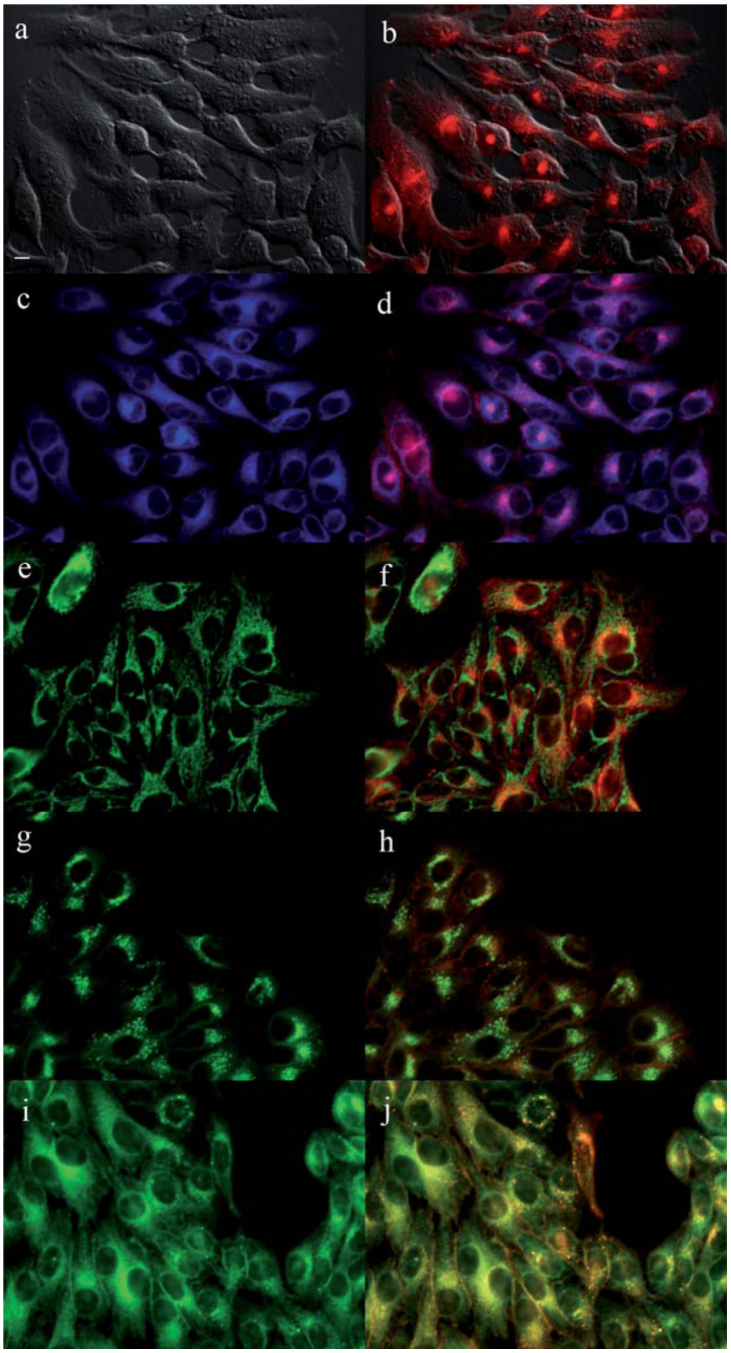

Fig. 3.

Subcellular localization of Pc **4a** in HEp2 cells at 10 μM for 6 h: (a) Phase contrast, (b) Overlay of **4a** and phase contrast, (c) ER tracker Blue/White fluorescence, (e) MitoTracker Green fluorescence, (g) BoD-IPY Ceramide, (i) LysoSensor Green fluorescence, and (d, f, h, j) overlays of organelle tracers with compound fluorescence. Scale bar: 10 μm.

NIH-PA Author Manuscript
NIH-PA Author Manuscript
NIH-PA Author Manuscript

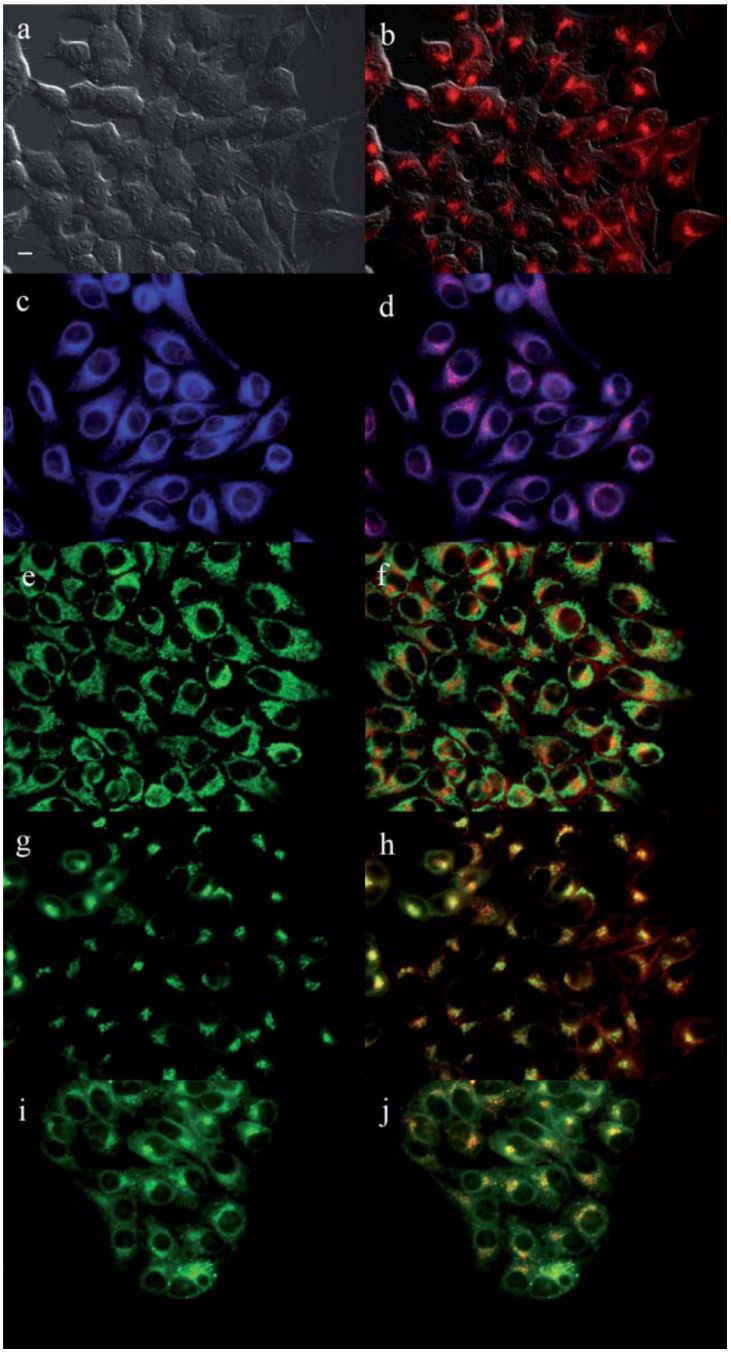

Fig. 4.

Subcellular localization of Pc **4b** in HEp2 cells at 10 μM for 6 h: (a) Phase contrast, (b) Overlay of **4b** and phase contrast, (c) ER tracker Blue/White fluorescence, (e) MitoTracker Green fluorescence, (g) BoD-IPY Ceramide, (i) LysoSensor Green fluorescence, and (d, f, h, j) overlays of organelle tracers with compound fluorescence. Scale bar: 10 μm.

NIH-PA Author Manuscript
NIH-PA Author Manuscript
NIH-PA Author Manuscript

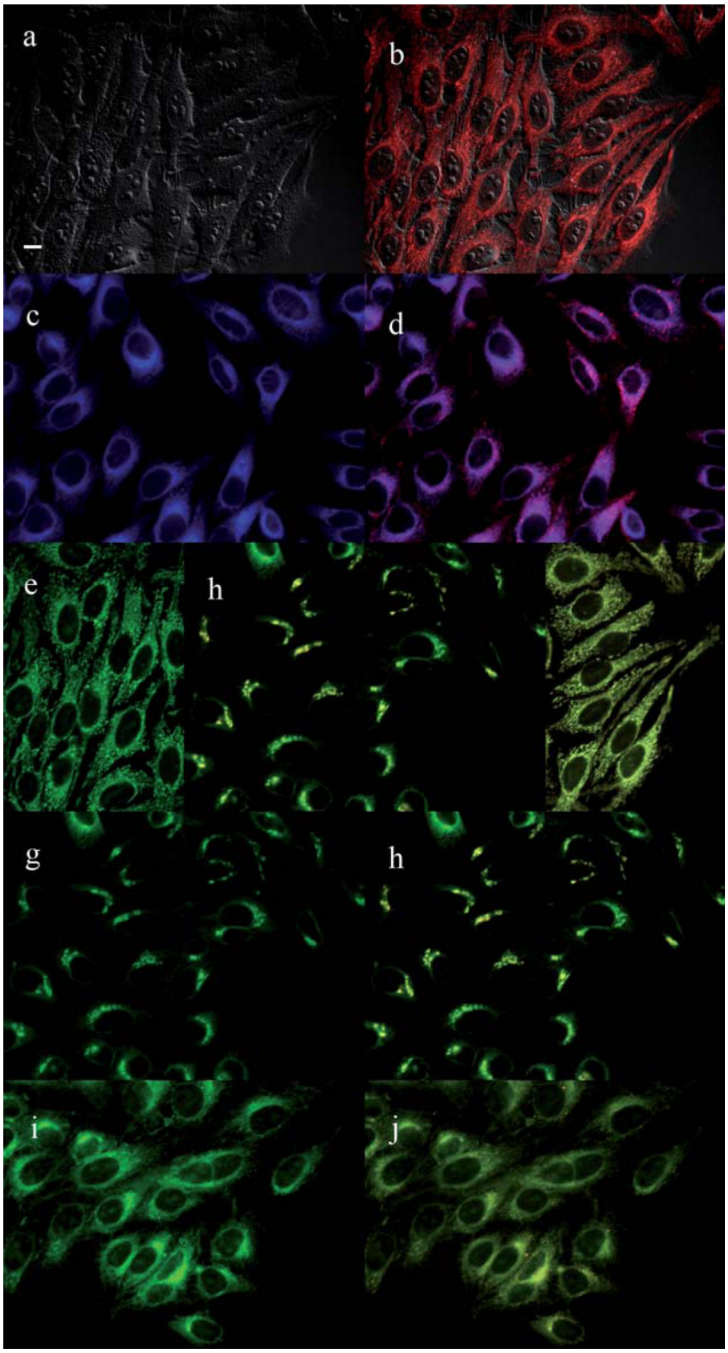

Fig. 5.

Subcellular localization of Pc **6a** in HEp2 cells at 10 μM for 6 h: (a) Phase contrast, (b) Overlay of **6a** and phase contrast, (c) ER tracker Blue/White fluorescence, (e) MitoTracker Green fluorescence, (g) BoD-IPY Ceramide, (i) LysoSensor Green fluorescence, and (d, f, h, j) overlays of organelle tracers with compound fluorescence. Scale bar: 10 μm.

NIH-PA Author Manuscript
NIH-PA Author Manuscript
NIH-PA Author Manuscript

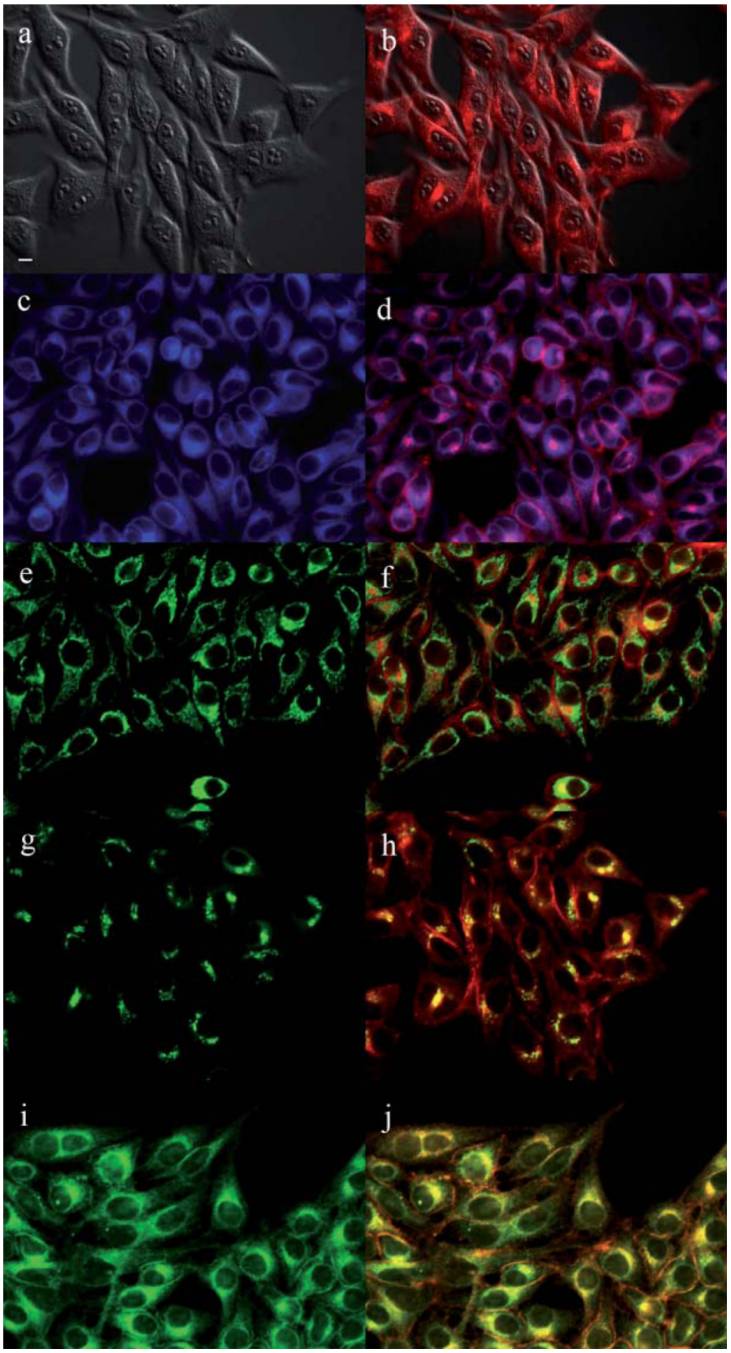

Fig. 6.

Subcellular localization of Pc **6b** in HEp2 cells at 10 μM for 6 h: (a) Phase contrast, (b) Overlay of **6b** and phase contrast, (c) ER tracker Blue/White fluorescence, (e) MitoTracker Green fluorescence, (g) BoD-IPY Ceramide, (i) LysoSensor Green fluorescence, and (d, f, h, j) overlays of organelle tracers with compound fluorescence. Scale bar: 10 μm.

NIH-PA Author Manuscript

NIH-PA Author Manuscript

NIH-PA Author Manuscript

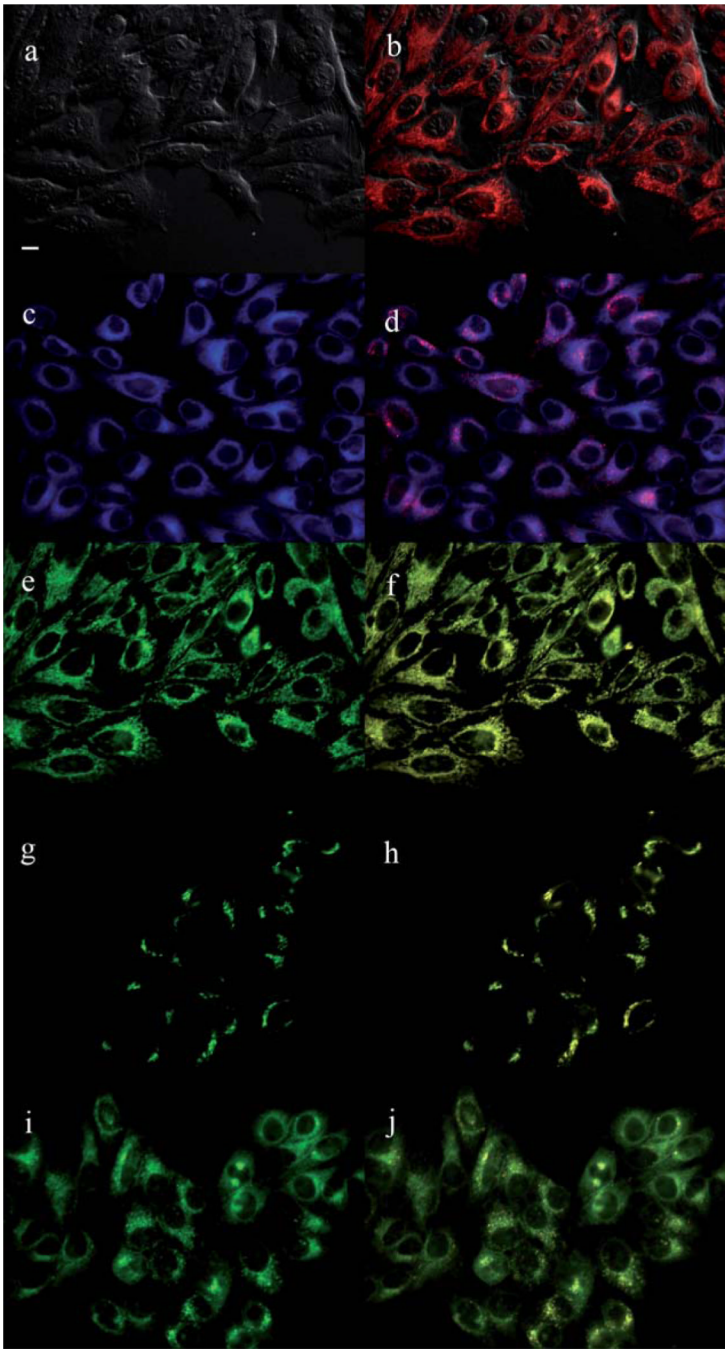

Fig. 7.

Subcellular localization of Pc **8** in HEp2 cells at 10 μM for 6 h: (a Phase contrast, (b) Overlay of **8** and phase contrast, (c) ER tracker Blue White fluorescence, (e) MitoTracker Green fluorescence, (g) BoDIP Ceramide, (i) LysoSensor Green fluorescence, and (d, f, h, j) overlays o organelle tracers with compound fluorescence. Scale bar: 10 μm.

NIH-PA Author Manuscript

NIH-PA Author Manuscript

NIH-PA Author Manuscript

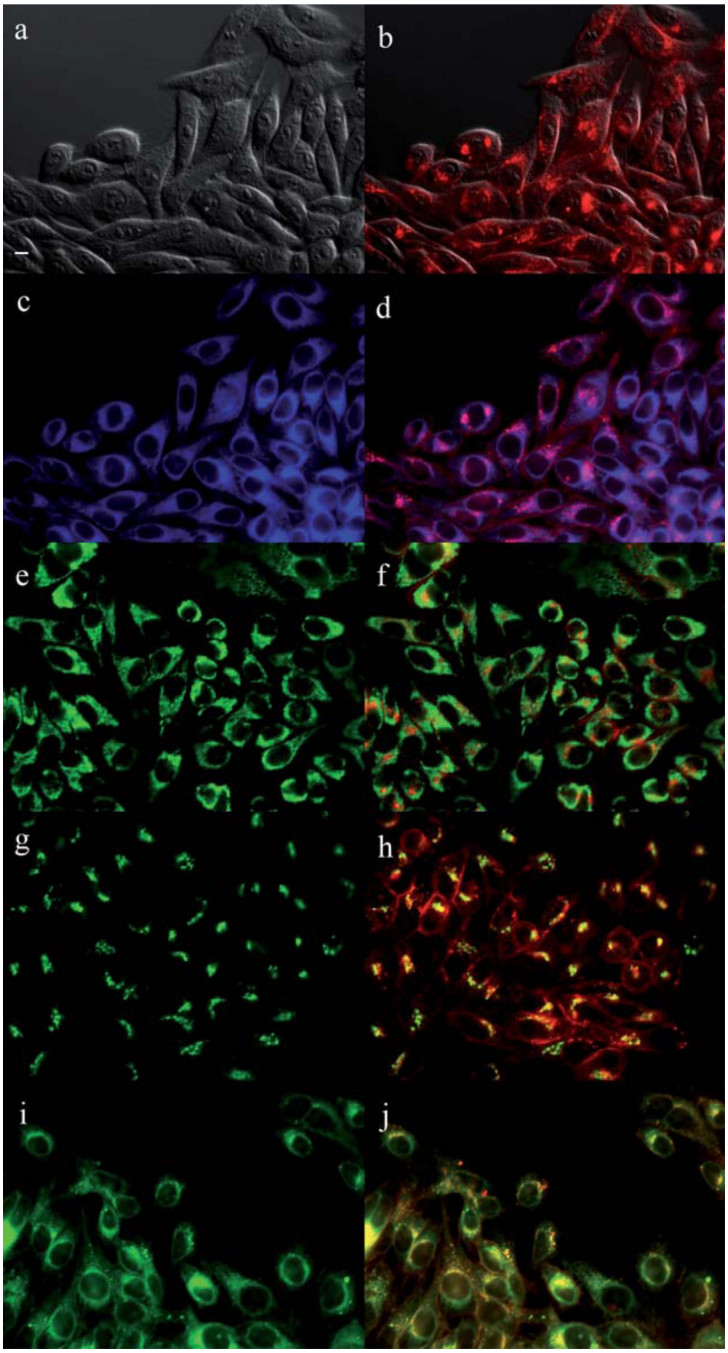

Fig. 8.

Subcellular localization of Pc **12** in HEp2 cells at 10 μM for 6 h: (a) Phase contrast, (b) Overlay of **12** and phase contrast, (c) ER tracker Blue/White fluorescence, (e) MitoTracker Green fluorescence, (g) BoD-IPY Ceramide, (i) LysoSensor Green fluorescence, and (d, f, h, j) overlays of organelle tracers with compound fluorescence. Scale bar: 10 μm.

NIH-PA Author Manuscript

NIH-PA Author Manuscript

NIH-PA Author Manuscript

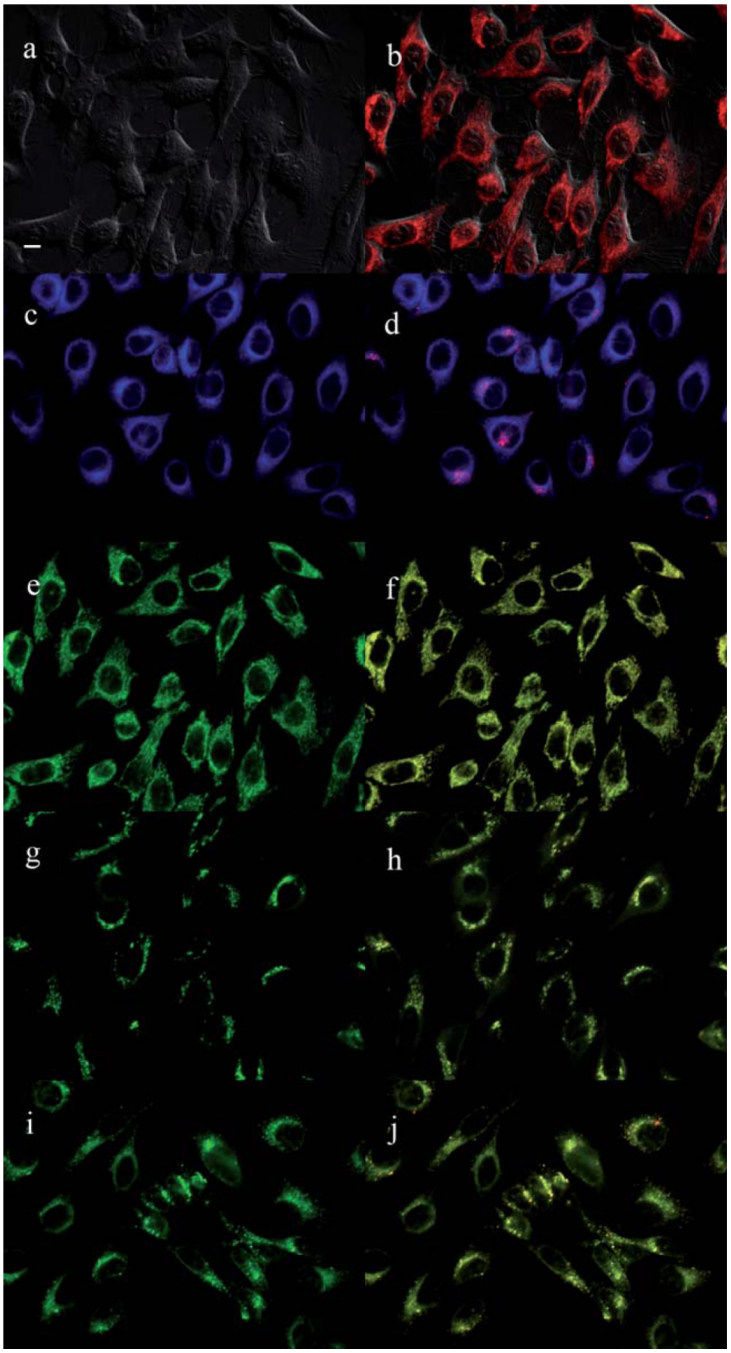

Fig. 9.

Subcellular localization of Pc **14** in HEp2 cells at 10 μM for 6 h: (a) Phase contrast, (b) Overlay of **14** and phase contrast, (c) ER tracker Blue/White fluorescence, (e) MitoTracker Green fluorescence, (g) BoD-IPY Ceramide, (i) LysoSensor Green fluorescence, and (d, f, h, j) overlays of organelle tracers with compound fluorescence. Scale bar: 10 μm.

NIH-PA Author Manuscript
NIH-PA Author Manuscript
NIH-PA Author Manuscript

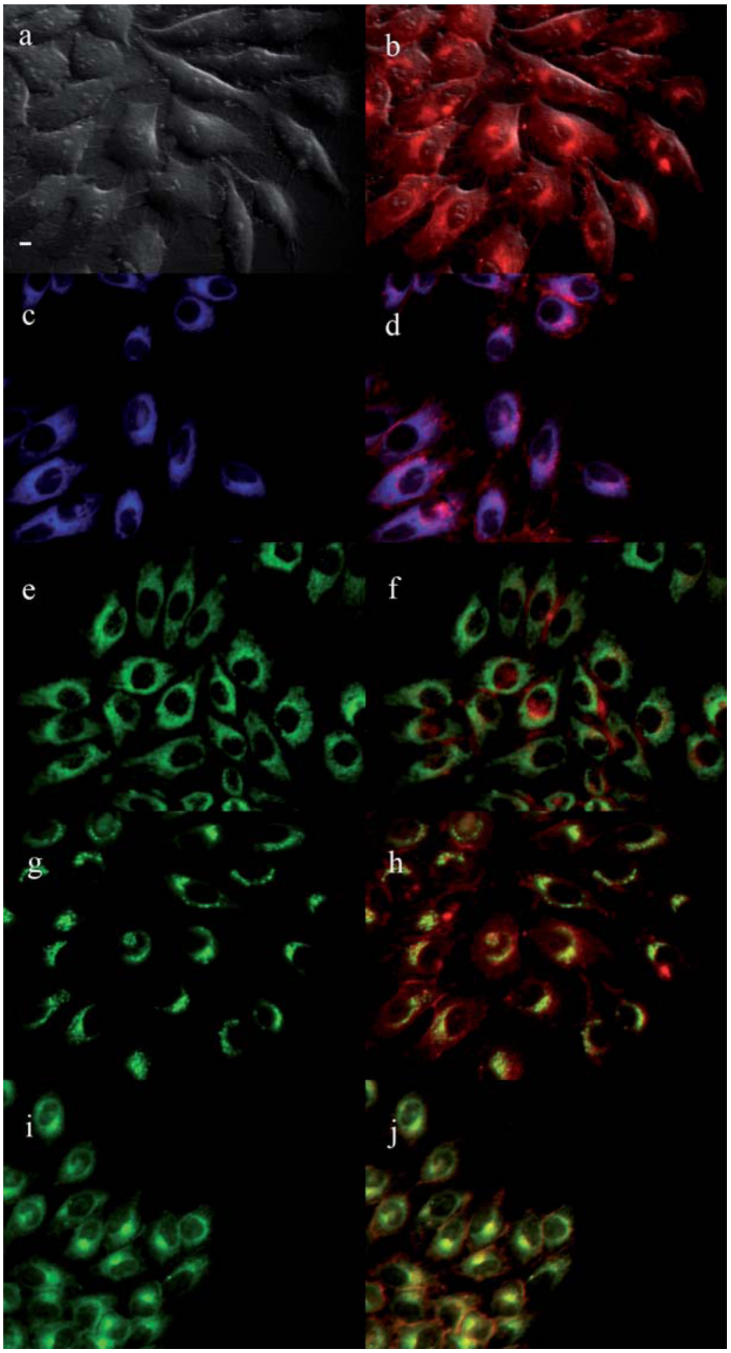

Fig. 10.

Subcellular localization of Pc **17a** in HEp2 cells at 10 μM for 6 h: (a) Phase contrast, (b) Overlay of **17a** and phase contrast, (c) ER tracker Blue/White fluorescence, (e) MitoTracker Green fluorescence, (g) BoD-IPY Ceramide, (i) LysoSensor Green fluorescence, and (d, f, h, j) overlays of organelle tracers with compound fluorescence. Scale bar: 10 μm.

NIH-PA Author Manuscript
NIH-PA Author Manuscript
NIH-PA Author Manuscript

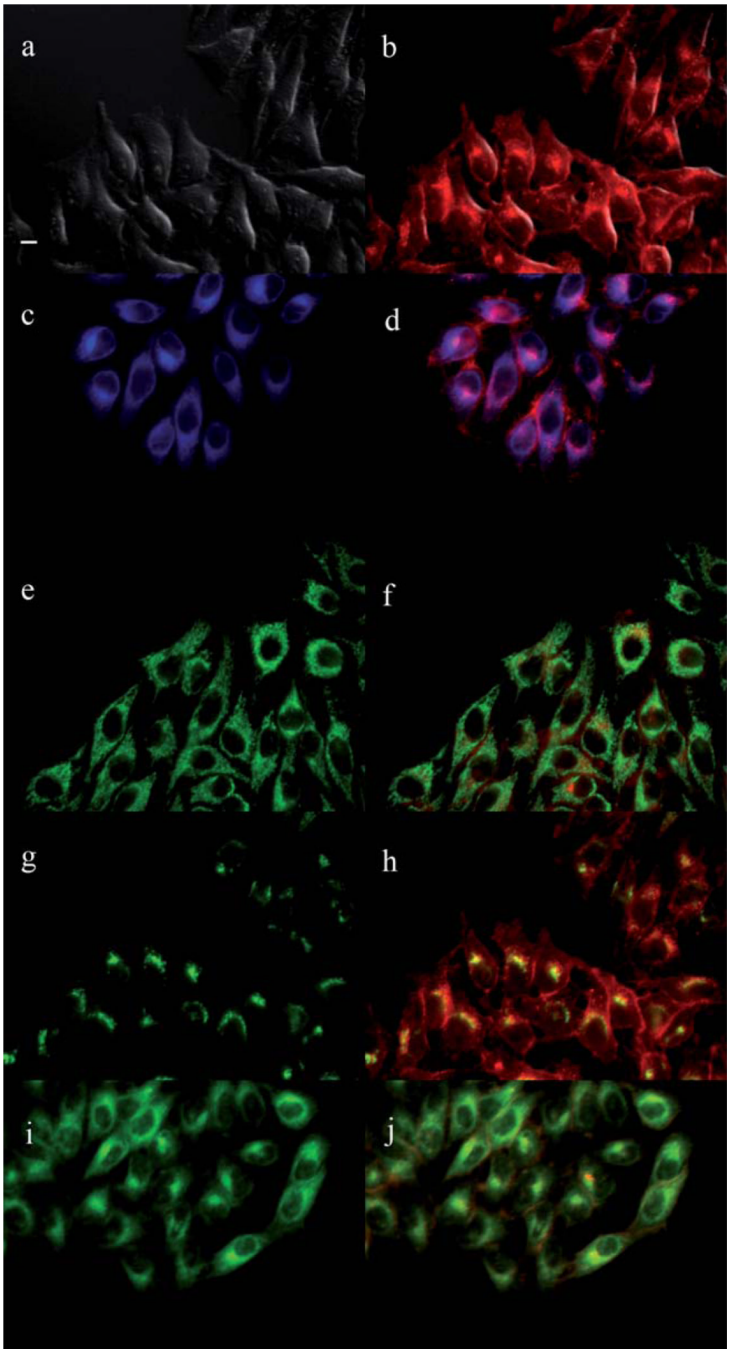

Fig. 11.

Subcellular localization of Pc **17b** in HEp2 cells at 10 μM for 6 h: (a) Phase contrast, (b) Overlay of **17b** and phase contrast, (c) ER tracker Blue/White fluorescence, (e) MitoTracker Green fluorescence, (g) BoD-IPY Ceramide, (i) LysoSensor Green fluorescence, and (d, f, h, j) overlays of organelle tracers with compound fluorescence. Scale bar: 10 μm.

NIH-PA Author Manuscript
NIH-PA Author Manuscript
NIH-PA Author Manuscript

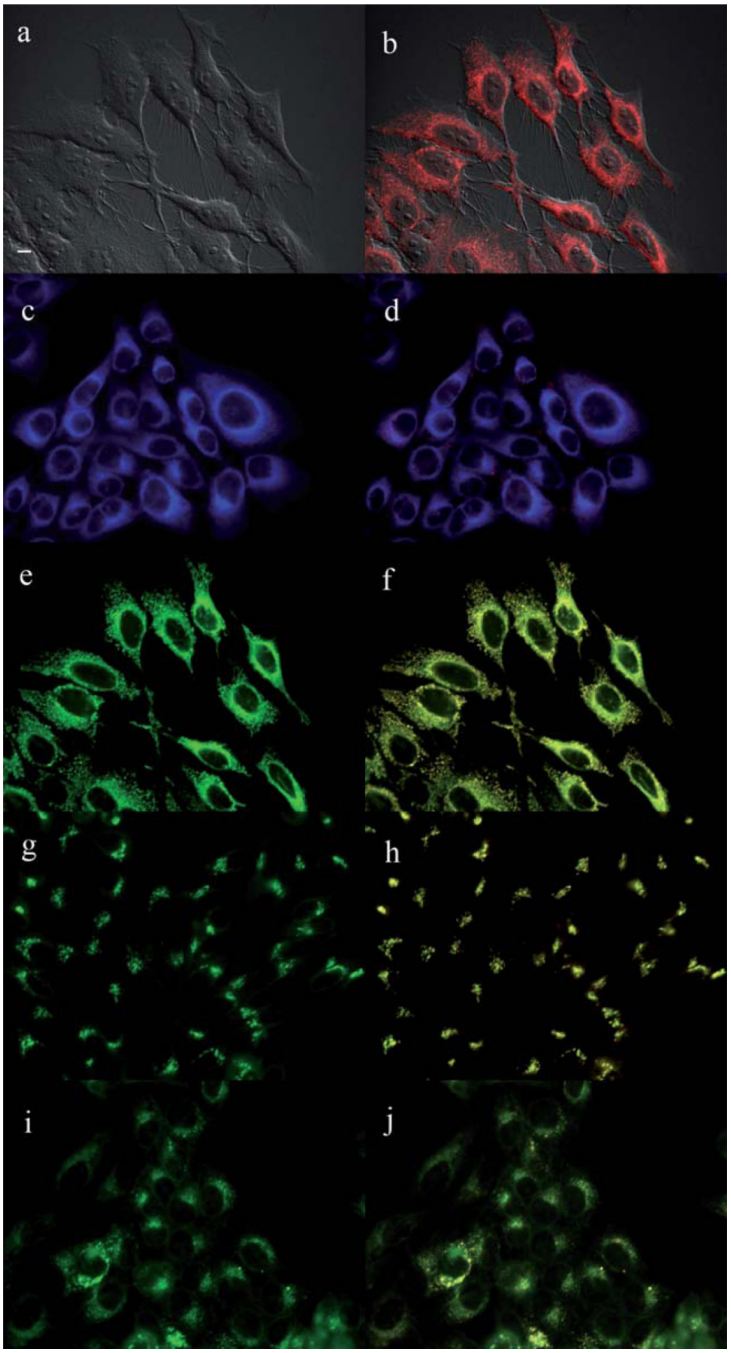

Fig. 12.

Subcellular localization of Pc **13** in HEp2 cells at 10 μM for 6 h: (a) Phase contrast, (b) Overlay of **13** and phase contrast, (c) ER tracker Blue/White fluorescence, (e) MitoTracker Green fluorescence, (g) BoD-IPY Ceramide, (i) LysoSensor Green fluorescence, and (d, f, h, j) overlays of organelle tracers with compound fluorescence. Scale bar: 10 μm.

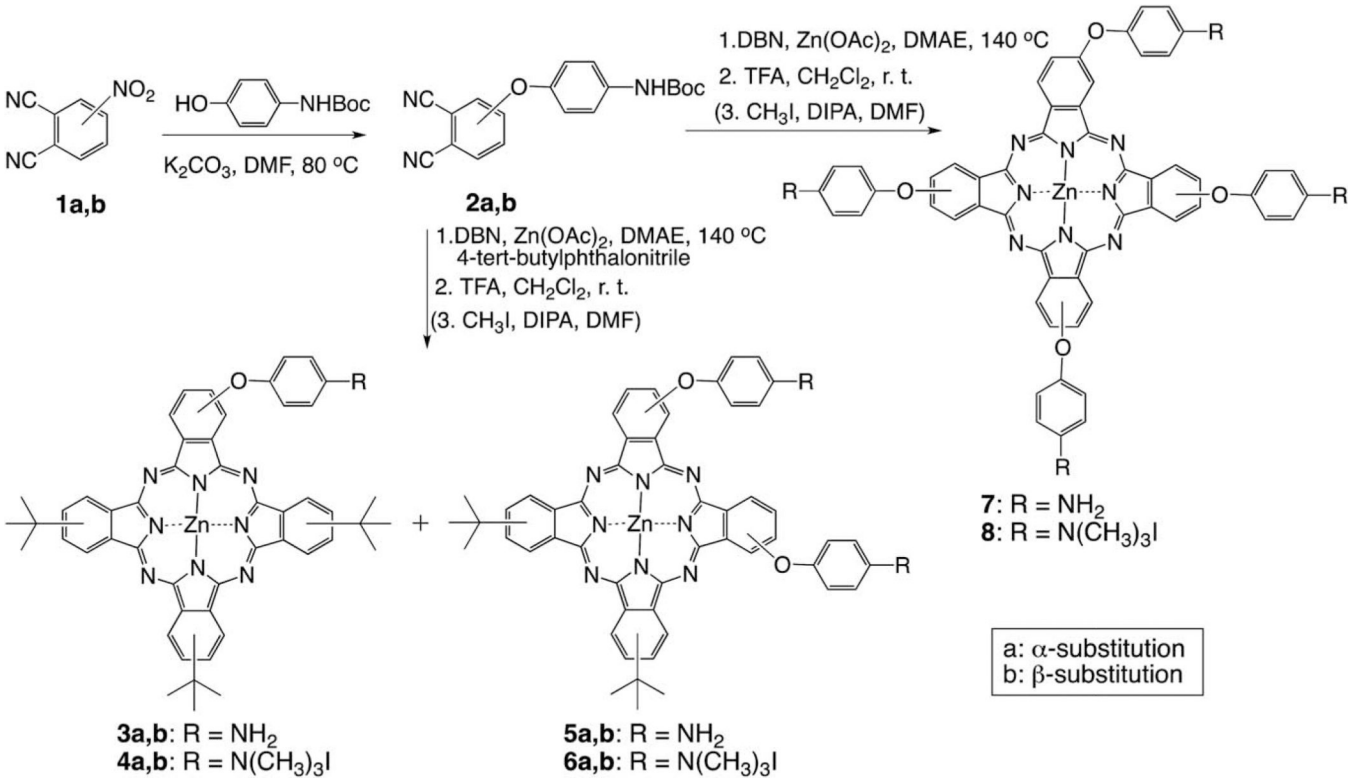

Scheme 1.
Synthesis of mono-, di- and tetra-cationic Pcs.

NIH-PA Author Manuscript NIH-PA Author Manuscript NIH-PA Author Manuscript

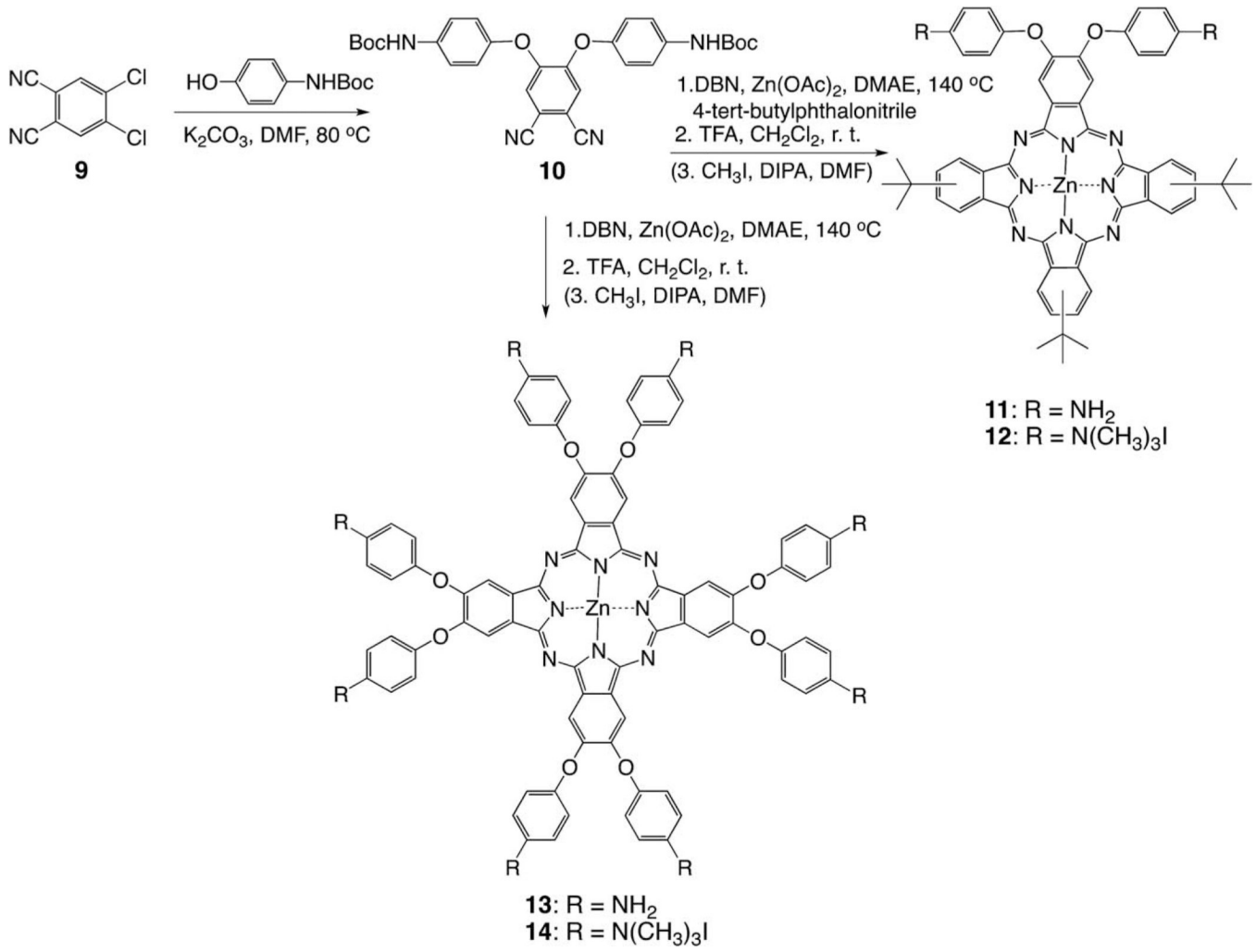

Scheme 2.
Synthesis of β-substituted di- and octa-cationic ZnPcs.

NIH-PA Author Manuscript NIH-PA Author Manuscript NIH-PA Author Manuscript

NIH-PA Author Manuscript

NIH-PA Author Manuscript

NIH-PA Author Manuscript

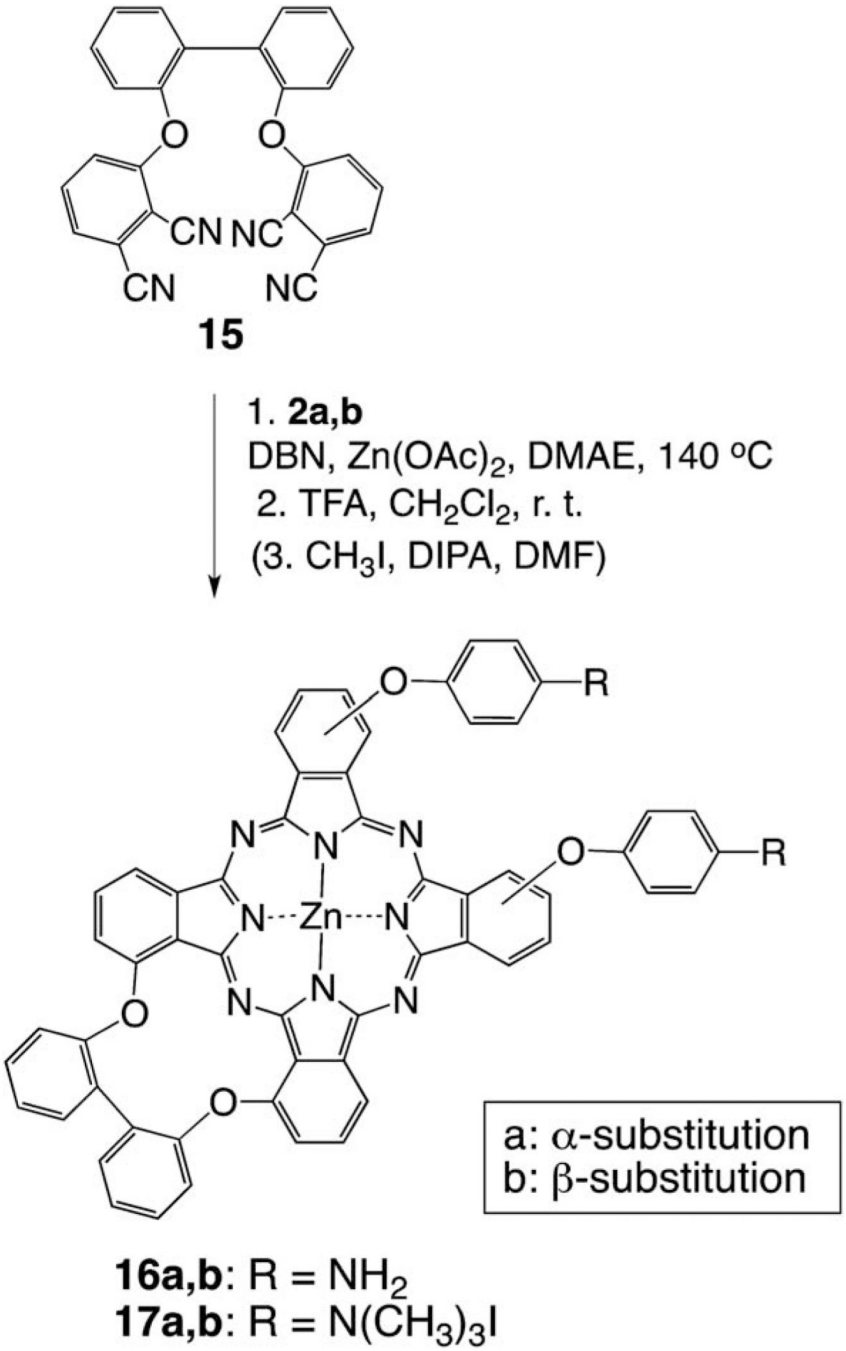

Scheme 3.
Synthesis of *cis*-A_2B_2 di-cationic ZnPcs.

NIH-PA Author Manuscript
NIH-PA Author Manuscript
NIH-PA Author Manuscript

Table 1

Spectral properties of ZnPcs **4, 6, 8, 12, 14** and **17** in DMF at room temperature

ZnPc	Absorption λ_{max} (nm)	Emission[a] λ_{max} (nm)	Stokes' shift (nm)	Φ_f[b]	Φ_Δ[c]
4a	684	686	2	0.16	0.47
4b	683	687	4	0.13	0.33
6a	686	689	3	0.21	0.31
6b	683	686	3	0.18	0.44
8	684	687	3	0.13	0.35
12	684	687	3	0.19	0.16
14	686	688	2	0.13	0.28
17a	685	687	2	0.11	0.33
17b	680	682	2	0.14	0.22

[a] Excitation at 640 nm.

[b] Calculated using ZnPc (Φ_f =0.17) as the standard.

[c] Calculated using ZnPc (Φ_Δ= 0.56) as the standard in DMF.

Medchemcomm. Author manuscript; available in PMC 2012 February 1.

NIH-PA Author Manuscript

NIH-PA Author Manuscript

NIH-PA Author Manuscript

Table 2

Dark and phototoxicity (at 1.5 J cm^{-2} light dose) of ZnPcs toward HEp2 cells using the Cell Titer Blue assay

ZnPc	Dark toxicity IC_{50} (μM)	Phototoxicity IC_{50} (μM)	Ratio
4a	>400	46.3	>9
4b	>400	>100	>4
6a	344	2.7	128
6b	156	13.4	12
8	>400	>100	>4
12	>400	39.6	>10
13	>400	>100	>4
14	>400	>100	>4
17a	>400	2.7	>148
17b	>400	12.1	>33